Report of Cooperative Education

Feasibility Study of Hydrogen Recovery from Hydrogenation Process

Siwat Valeekiatkul

A Report Submitted in Partial Fulfillment of the Requirements for the Degree of Bachelor of Engineering (Petrochemical Engineering), Department of Chemical Engineering, Faculty of Engineering, King Mongkut's Institute of Technology Ladkrabang

Academic Year 2016

Cooperative Title:	Feasibility Study of Hydrogen Recovery from Hydrogenation Process
By:	Mr. Siwat Valeekiatkul
Field of Study:	Bachelor Degree in Chemical Engineering in Petrochemical Program
Advisor:	Assoc. Prof. Dr. Anchaleeporn Waritswat Lothongkum
Co-advisor:	Dr. Narisara Thongboonchoo
Mentor (Position):	Mr. Songpon Puangpimol (Project Engineering)
Company:	Siam Mitsui PTA Co., Ltd.

Abstract

The production of purified terephthalic acid (PTA) consists of CTA (Crude Terephthalic Acid) unit and PTA unit. PTA is raw material of polyester and polyethylene terephthalate (PET) production. The oxidation between *p*-xylene and oxygen occurs in CTA unit by using Co/Mn catalyst. Main impurity of the CTA unit is 4-carboxy benzaldehyde (4-CBA). Therefore, CTA powder is purified by hydrogenation process in the PTA unit, and 4-CBA is converted to para-toluic acid (*p*-TA) by using Pd/C catalyst. *p*-TA is subsequently separated by liquid-liquid extraction. In the PTA unit, CTA slurry and excess hydrogen are fed into hydrogenation process. The remaining hydrogen is dissolved in PTA slurry. Crystallizers are used to separate steam and hydrogen from PTA slurry. Steam and hydrogen are sent to the exchanger. It was found that hydrogen of about 108 Nm^3/h (5.3 MBaht/year) lost at the ventilation line of the exchanger. Therefore, hydrogen recovery unit (HRU) is required. In regard to high % hydrogen purity, high % hydrogen recovery and low investment cost, the pressure swing adsorption (PSA) is selected. Apart from 4-CBA and *p*-TA, water and benzoic acid (BA) are found in the CTA unit. The condenser and scrubber are required for pre-treatment of water and BA, respectively. Hence, the deisgn process in this work for pre-treatment of the impurities and hydrogen recovery are condenser, scrubber and 4 vessels of pressure swing adsorption, which operates at 50 °C and 35 bar. Hydrogen (99.99 %purity, 5.7 kg/h) of approximately 85 wt% was recovered. The estimated saving cost is 3.8 MBaht/year.

Keywords: PTA, Hydrogenation, Hydrogen Recovery, Pressure Swing Adsorption

Acknowledgements

I would like to thank Siam Mitsui PTA Co., Ltd., for providing me an opportunity to do my co-operative education project on "Feasibility Study of Hydrogen Recovery from Hydrogenation Process" of chemical engineering (petrochemical program). It was a great chance for learning and professional development.

I sincerely thank Mr. Songpol Puangpimol, Project Engineering, who encouragement in carrying out this thesis project work. I also wish to express my gratitude to Mr. Sitthichai Tangsatjatham, Engineering Manager, and Mr. Piya Panichayunon, Project Engineering, who gave me the suggestions, and engineering skills. I also thank to operator staff of PTA production plant 3 who provided the assistant.

In addition, I am highly indebted to my advisor Assoc. Prof. Dr. Anchaleeporn Waritswat Lothongkum for her guidance and constant supervision as well as for providing necessary information regarding the project and also for her support in completing the project. Besides my advisor, I wish to express my sincere gratitude to my co-advisor, Dr. Narisara Thongboonchoo, who gave me the comments, providing the knowledge and support me throughout this thesis project.

Finally, I would like to thank my family, my teachers and my friends who always be the backup and be hide every success of me.

Siwat Valeekiatkul

Table of Contents

Table of Contents

Table of Contents

List of Figures

List of Figures

List of Tables

Nomenclature

A is heat transfer area

c_0 is initial concentration

c_b is break-point concentration

C_p is fluid specific heat, heat capacity

D_b is bundle diameter

D_c is column diameter

D_s is shell indside diameter

d_e is equivalent diameter ($d_e = \frac{4 \times cross\ section\ area\ for\ flow}{wetted\ perimeter} = d_i\ for\ tubes$)

d_i is tube inside diameter

d_o is tube outside diameter

F_t is the temperature correction factor

f_1 is liquid viscosity correction factor ($(\frac{\mu_L}{\mu_w})^{0.16}$)

f_2 is density correction factor ($(\frac{\rho_w}{\rho_L})^{1.25}$)

f_3 is surface tension correction factor ($(\frac{\sigma_w}{\sigma_L})^{0.8}$)

f_i is inside dirt coefficient

f_o is outside dirt coefficient (fouling factor)

F_p is the packing factor

G_m is molar gas flow rate per unit cross-sectional area

g is gravitational accretion

H_G is height of a gas-phase transfer unit

H_L is height of a liquid-phase transfer unit

H_{OG} is the height of an overall gas-phases transfer unit

H is the Henry's law constant in atm/mole fraction for the given system

H_B is the length of bed used up to the break point

h_i is inside fluid film coefficient

h_o is outside fluid film coefficient

H_T is total bed length

H_{UNB} is length of unused bed

K_3 is percentage flooding correction factor

k_f is fluid thermal conductivity

k_L is condensate thermal conductivity

k_w is thermal conductivity of the tube wall material

L' is kg mol inert liquid/s or kg mol inert liquid/s $\times$ m^2

L_W^* liquid mass flow rate per unit area column cross-section area

L_m is molar liquid flow rate per unit cross-sectional area

l_B is baffle spacing

L is tube length

m is the slope of the equilibrium line

N_{OG} is the number of overall gas-phases transfer units

N_p is number of tube side passes

N_t is number of tubes

N_r is average number of tubes in a vertical tube row

N_t is total number of tubes in the bundle

Nu is Nusselt number ($\frac{h_i d_e}{k_f}$)

ΔP_s is tube side pressure drop

p_t is tube pitch

$\Delta P_{flood}$is in in. H_2O/ft height of packing

p_A is partial pressure of substance A

Pr is Prandtl number ($\frac{C_p \mu}{k_f}$)

p_t is tube pitch

$Q_{crystalline}$ is energy crystallization of PTA

Q_{in} is energy flow in crystallizer by CTA slurry

$Q_{out}$is energy flow out of crystallizer

Q_{purge} is energy flow in crystallizer by purge water

Q_{total} is overall energy balance at crystallizer

$Q_{vaporlize}$ is energy vaporization of water

$Q_{Cold\ side}$ is energy of cold side

$Q_{Hot\ side}$ is energy of hot side

Q is heat transferred per unit time

R is equal to the shell side fluid flow-rate times the fluid mean specific heat divided by the tube side fluid flow rate times the tube side fluid specific heat

Re is Reynolds number ($\frac{\rho d_e u_s}{\mu}$)

S is a measure of the temperature efficiency of the exchanger

Sc_L is liquid Schmidt number ($\frac{\mu_L}{\rho_L \times D_L}$)

Sc_v is gas Schmidt number ($\frac{\mu_v}{\rho_g \times D_v}$)

T_1 is hot fluid temperature inlet

T_2 is hot fluid temperature outlet

t_1 is cold fluid temperature inlet

t_2 is cold fluid temperature outlet

ΔT_{lm} is log mean temperature difference.

ΔT_m is the true temperature difference from logarithmic mean temperature

t_b is break-point time

t_t is total adsorption time

t_t is the time equivalent to the total or stochiometric capacity.

t_u is the time equivalent to usable capacity or the

u_t is tube side velocity

U is overall heat transfer coefficient

V' is kg nol inert gas/s or kg mol inert gas/s $\times$ m^2

W_s is fluid flow rate on the shell side

W_c is total condensate flow

x is mole fraction of solute in liquid

x_A is mole fraction of solute in liquid

y is mole fraction of solute in gas

Z is column height

Greek

Ψ_h is H_G factor

μ_L is condensate viscosity

μ_w is fluid viscosity at the wall

ρ is shell side fluid density

ρ_L is condensate density

ρ_v is vapor density

ϕ_h is H_L factor

Γ is the tube loading, the condensate flow per unit length of tube ($\Gamma_h = \frac{Wc}{L \times N_t}$)

μ is fluid viscosity at the bulk fluid temperature

CHAPTER I
INTRODUCTION

1.1 Background

Siam Mitsui PTA Co., Ltd. (SMPC) is a joint venture between SCG Chemical Co., Ltd. and Mitsui Chemical Inc. from Japan which produces PTA (Purified Terephthalic Acid). PTA is the white powder, It is the main source of polyester and PET (Polyethylene Terephthalate) which are the main raw material for textile and bottle grades production, respectively. There are 2 units, CTA (Crude Terephthalic Acid) unit and PTA unit to produce PTA powder. The oxidation between para-xylene and oxygen occurs in CTA unit by using Co/Mn and Br being catalyst and promoter, respectively. Including acetic acid which is the solvent to produce CTA powder. CTA powder is mixed with impurities such as 4-caboxy benzaldehyde (4-CBA) and others. The 4-CBA effects on average molecular weight of the polymer and the rate of polymerization as well. Therefore, CTA powder need to be purified by hydrogenation reactor in PTA unit. It operates by using Pd/C as a catalyst to convert the major impurity, 4-CBA to be para-toluic acid (p-TA) which can be separated by liquid-liquid extraction because of the *p*-TA solubility property. In hydrogenation reactor, the CTA slurry and excess hydrogen are fed into hydrogenation reactor. The remaining hydrogen will dissolve in slurry and send to crystallizer for separating; consequently, the hydrogen will loss at the vent of exchanger around 108 Nm^3/h which calculate to the loss cost around 5.3 MBath/Year. So, it is the reason why I interested to study the hydrogen recovery unit which is suitable for PTA plant.

1.2 Objective

To study feasibility of H_2 recovery in PTA plants.

1.3 Scope of the Project

1.3.1 Study hydrogen loss in PTA plants.

1.3.2 Study technique and technology to recover hydrogen.

1.3.3 Design new process to recover hydrogen.

1.4 Expected Outputs

1.4.1 Understanding in PTA unit operation.

1.4.2 Understanding in process design of absorption unit, heat exchanger unit and pressure swing adsorption unit.

CHAPTER II
LITERATURE REVIEW

2.1 Purified Terephthalic Acid Production

[Abbas Azarpour, S. Tourani, Zhi Li]

Normally, purified terephthalic acid (PTA) production is the production from Amoco Chemical Company which has been proposed in the past decade. PTA is used for production of polyester and polyethylene terephthalate (PET) which are variety used in industries production of film, fiber and drinking bottles, respectively.

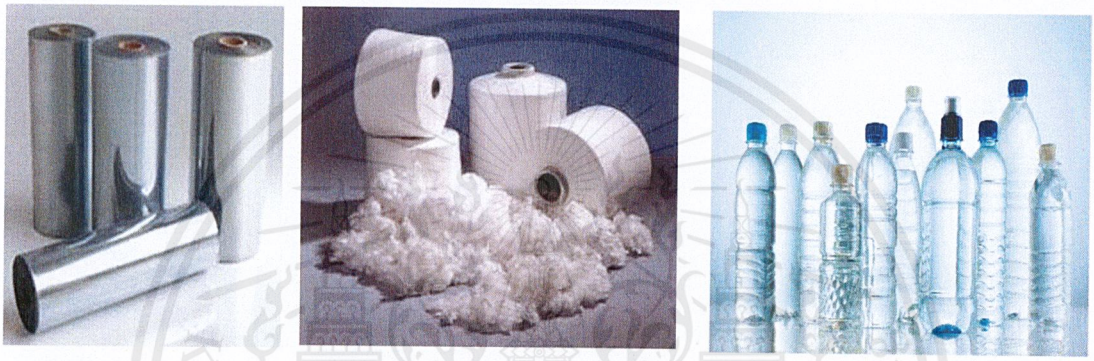

(a) (b) (c)

Figure 2.1 Products from PTA: (a) Polyester Film, (b) Polyester Fiber and (c) PET bottles [Yoo Huat Co., Ltd., Mazharul Islam Kiron, 2016]

2.1.1 CTA Process

The manufacturing and purifying of PTA involves two stages: in the first stage para-xylene is oxidized to form crude terephthalic acid (CTA) by using Co/Mn and Br being catalyzed as well as acetic acid which is a solvent to produce CTA powder.

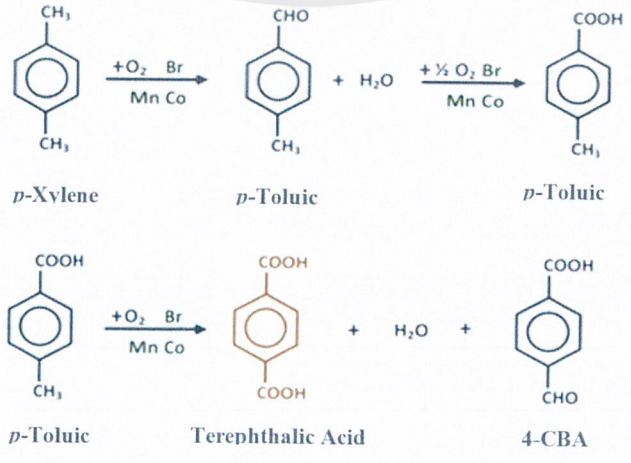

Figure 2.2 PTA production by oxidation [Johnson Matthey, 2016]

The most common industrial process for manufacturing CTA is oxidized para-xylene at a temperature about 176 to 225 ^{O}C and a pressure about 1500 to 3000 kPa. The resulting product that calls CTA contains about 3000 ppm of 4-carboxybenzaldyhyde (4-CBA) and 500 ppm of *p*-toluic acid as the major impurities.

2.1.2 PTA Process

Hydrogenation offers the easiest route for removal of 4-carboxybenzaldehyde (4-CBA) impurity from the crude terephthalic acid (TA). This invention is improved for the hydrogenation process of crude terephthalic acid that is a catalyst prepared by utilizing palladium metal deposited upon an active carbon support. 4-CBA and *p*-toluic acid do not have two carboxylic acid groups and would thus terminate the chain reaction for polyester production from CTA. 4-CBA is also yellow in color and its presence in CTA would result in a colored product with a lower average molecular weight that is undesired in fiber manufacturing. Compared with 4-CBA, *p*-toluic acid is only produced in small quantities and since it is water soluble (Table 2.1), it is easily removed in a crystallization step. The permissible concentrations of 4-CBA in PTA as a polyester feed stock is usually less than 25 ppm.

Table 2.1 Solubility (g/100 mlH_2O) of different compounds in water [Siam Mitsui PTA Co., Ltd., 2016]

Compound	At 20 ^{O}C	At 100 ^{O}C
Benzoic Acid	0.5	100
p-Toluic Acid	0.34	6.8
4-CBA	0.005	0.25
TA	0.005	0.03

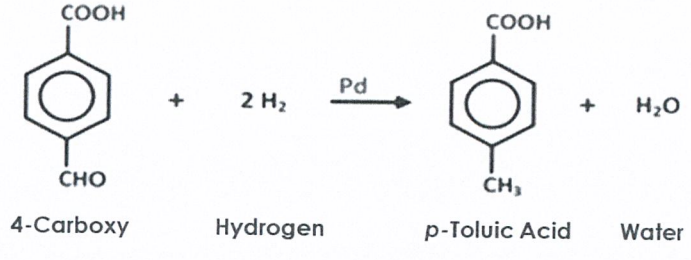

Figure 2.3 PTA production by hydrogenation [Johnson Matthey, 2016]

Hence, the hydrogenation reactor of PTA process use the hydrogen to reaction with 4-CBA. 4-CBA is converted to p-toluic acid which is water soluble. The

PTA production is control hydrogen pressure to make sure the conversion. Excess hydrogen is fed into the reactor. However, remaining hydrogen is accumulated in the pre-heater. So, ventilation gas line from pre-heater is used to solve low capacity due to gas accumulate. It will release to the ATM by stack (Figure 2.4).

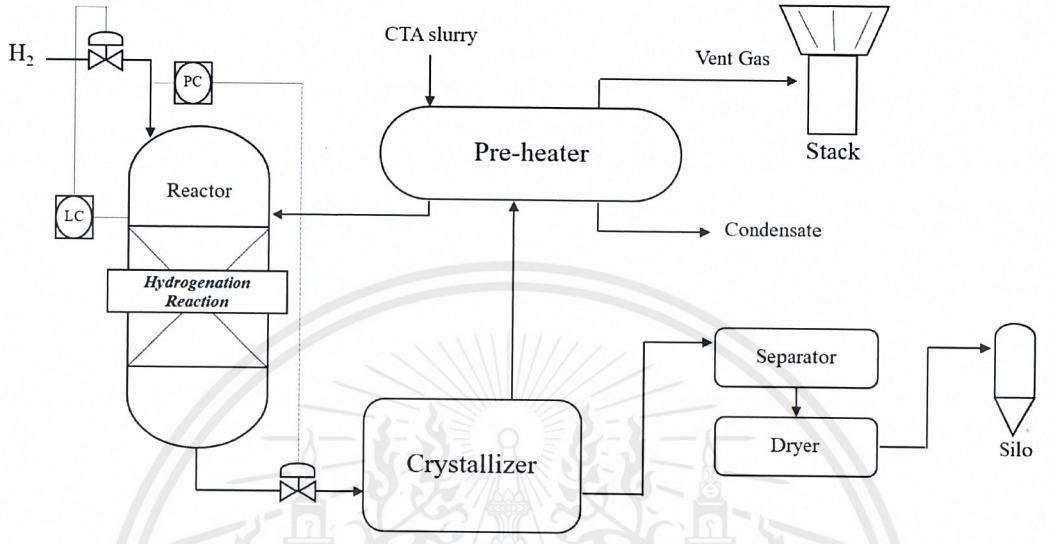

Figure 2.4 Hydrogenation process for PTA production
[Siam Mitsui PTA Co., Ltd., 2016]

Then, the resulting products pass through the series of flash crystallizers where temperature and pressure are sequentially decreased. All hydrogenation products therefore remain in the mother liquor while TA is crystallized out. The final PTA product has less than 25 ppm of 4-CBA as impurity.

2.2 Hydrogen Recovery Units [Itsuki Uehara, Ali Muvechain, Zajra Rabiei]

The processes in the removal of impurities from crude hydrogen to obtain a pure product can be roughly divided into three steps.

First step: is the pre-treatment of the crude hydrogen for the removal of specific contaminants that are detrimental to subsequent separation processes and for their conversion to easily separable species.

Second step: is the removal of both major and minor impurities to yield an acceptably pure hydrogen level.

Third step: is the final purification to a specified level.

The choice of a suitable separation process depends on the specifications and operating conditions of the feed and product gases. In the case of PTA production, the separation processes at the first and second steps mostly suffice. Typically, hydrogen purification technology includes pressure swing adsorption (PSA), membrane separation and cryogenic separation. For the purification technology, there is the varied rage for its operating parameters, such as temperature, pressure, %recovery, product composition and especially contaminants. The variation of these parameters, which is under the operator's control, affects the purifier's performance. However, each of these techniques have its unique and constraints. So, the suitably technology for PTA plant was chosen from studying by many patents, journal, books and others.

2.2.1 Pressure Swing Adsorption

[Christie John Geankoplis, Dong-Kyu Moon, The Linde Group, Coulson and Richardson's, 2016]

Pressure swing adsorption is the one of adsorption process type which is used for removing one or more components of a or liquid stream. It is removed by adsorb unwanted components (adsorbate) on the surface of the solid (adsorbent). In commercial processes, the adsorbent is usually in the form of small particles in a fixed bed. The stream line is passed through the bed and the solid particles adsorb unwanted components from the steam line. When the bed is almost saturated, the flow is changed to the other beds to adsorb unwanted. For the old bed, it is regenerated by using the pure product. However, it is normally regenerated by using thermal so that desorption occurs.

2.2.1.1 Physical Properties of Adsorbents

Many adsorbents have been developed for several years for a wide range of separations. Typically, the adsorbents are in the form of small pellets or beads. The ad sorption often occurs as a monolayer on the surface of the fine pores, although several layers sometimes occur. Physical adsorption, or van der Waals adsorption, usually occurs between the adsorbed molecules and the solid internal pore surface.

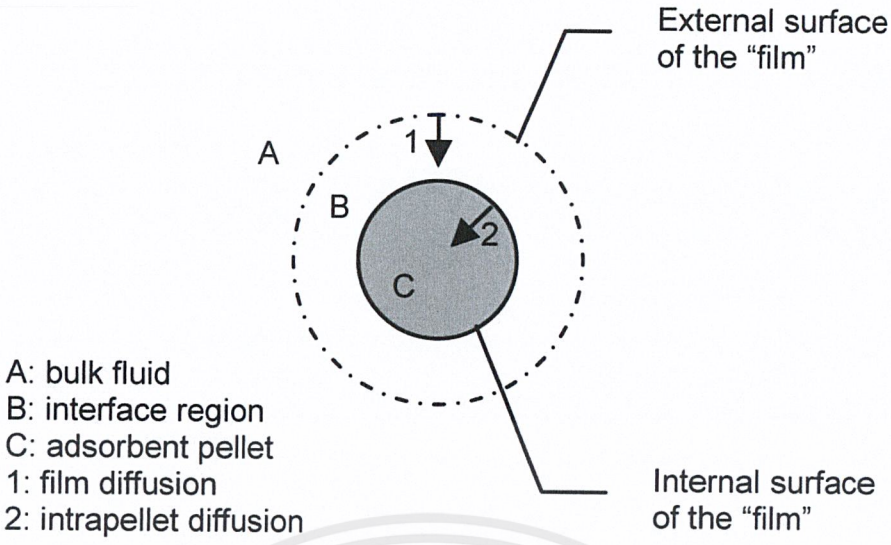

Figure 2.5 Adsorption process [Zhe Xu, 2013]

For the adsorption process, it has several steps which is in series as shown in Figure 2.5. When the fluid is flowing past the particle in a fixed bed, the solute first diffuses from the bulk fluid to the gross exterior surface of the particle. Then the solute diffuses inside the pore to the surface of the pore. Finally, the solute is adsorbed on the surface.

2.2.1.2 The Nature of Adsorbents

For the good adsorbents, it should have the highest surface area and lowest pressure drop for flow through the bed. To be attractive commercially, an adsorbent should embody these features.

1. It should have a large internal surface area.
2. The area should be accessible through pores big enough to admit the molecules to be adsorbed. It is a bonus if the pores are also small enough to exclude molecules which it is desired not to adsorb.
3. The adsorbent should be capable of being easily regenerated.
4. The adsorbent should not age rapidly, that is lose its adsorptive capacity through continual recycling.
5. The adsorbent should be mechanically strong enough to withstand the bulk handling and vibration that are a feature of any industrial unit.

2.2.1.3 Commercial Adsorbents

There are several commercial adsorbents which is chosen from several applications. If engineer choose wrong adsorbent for any application, adsorption process for separation will have the failure or cannot separate adsorbate from stream. So, the commercial adsorbents are described below.

1. **Activated carbon.** It is made by thermal decomposition of wood, vegetable shells, coal and others. It has surface areas of 300 to 1200 m^2/g with average pore diameter of 10 to 60 Angstrom. Activated carbon may be used as a powder which mixed with the liquid to be treated and then removed by filtration. It may also be used in granular form. When the use of carbon is low, it is normally economic to regenerate it.
2. **Silica gel.** This is made by acid treatment of sodium silicate solution and then drying. Unlike the activate carbons, the surface of silica gel is hydrophilic and it is commonly used for drying gases and also finds applications where there is requirement to remove unsaturated hydrocarbons.
3. **Activated alumina.** It is used when required high resistant to attrition. It is high capacity more than silica gel at higher temperatures. It is made by controlled heating of hydrated alumina. Activated alumina has a high affinity for water in particular and for hydroxyl groups in general. It cannot compete in terms of capacity or selectivity with molecular sieves although its superior mechanical strength is important in moving-bed applications.
4. **Molecular sieve (zeolites).** These zeolites are porous crystalline aluminosilicates that form an open crystal lattice congaing precisely uniform pores, which makes it different from other types of adsorbents. It has a rage of pore sizes. Zeolite are used for drying, separation of hydrocarbons, mixtures, and many other applications.
5. **Synthetic polymers (resins).** These are made by polymerizing two major types of monomers. Those made from aromatics such as styrene and divinylbenzene are used to adsorb nonpolar organics from aqueous solutions. Those made from acrylic esters are usable with more-polar solutes in aqueous solutions.

2.2.1.4 Basic Process of Pressure Swing Adsorption

Normally, pressure swing adsorption have minimal beds is 2 beds. However, for recovery hydrogen at least beds are 4 beds. In industrial operation, they use more than 4 beds because it should have spare bed for regenerate adsorbent when it has an accident and to provide continuous hydrogen supply as shown in Figure 2.6 and 2.7. So, basic process steps for 4 beds pressure swing adsorption are

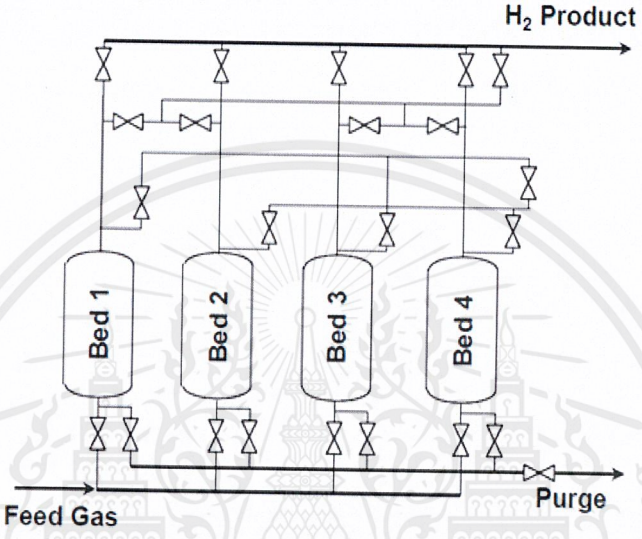

Figure 2.6 Pressure swing adsorption for recovery hydrogen [The Linde Group, 2016]

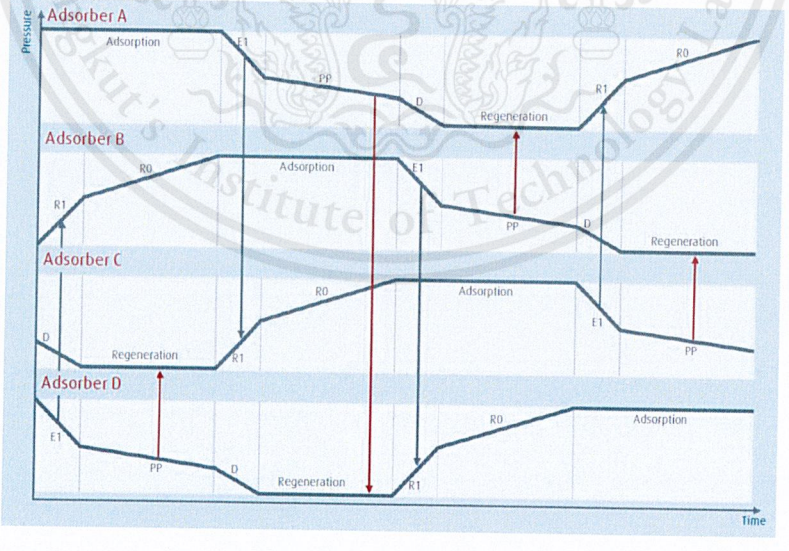

Figure 2.7 Pressure swing adsorption process diagram [The Linde Group, 2016]

2.2.1.4.1 Adsorption

Adsorption of impurities is carried out at high pressure being determined by the pressure of the feed gas. The feed gas flows through the adsorber

vessels in an upward direction. Impurities such as water, heavy hydrocarbons, light hydrocarbon, CO_2, CO and nitrogen are selectively adsorbed on the surface of the adsorbent material. High pure hydrogen exits the adsorber vessel at top. After a defined time, the adsorption phases of this vessel stop and regeneration starts. Another adsorber takes over the task of adsorption to ensure continuous hydrogen supply.

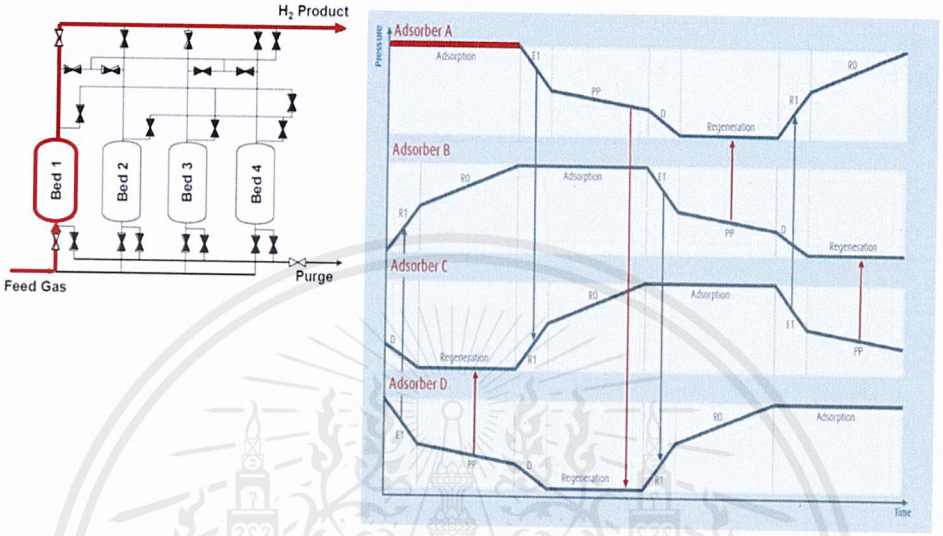

Figure 2.8 Adsorption step [The Linde Group, 2016]

2.2.1.4.2 Regeneration

The regeneration phase consists of basically five consecutive steps: pressure equalization, provide purge, dump, purging and repressurization. All of these steps are used for minimize hydrogen losses and consequently to maximize the hydrogen recovery rate of the pressure swing adsorption system.

1. Pressure Equalization (Step E1)

Depressurization starts in the co-current direction from bottom to top. The hydrogen still stored in the void space of the adsorbent material is used to pressurize another adsorber having just terminated its regeneration. Depending on the total number of adsorbers and the process conditions, one to four of these so-called pressure equalization steps are performed. Each additional pressure equalization step minimizes hydrogen losses and increases the hydrogen recovery rate.

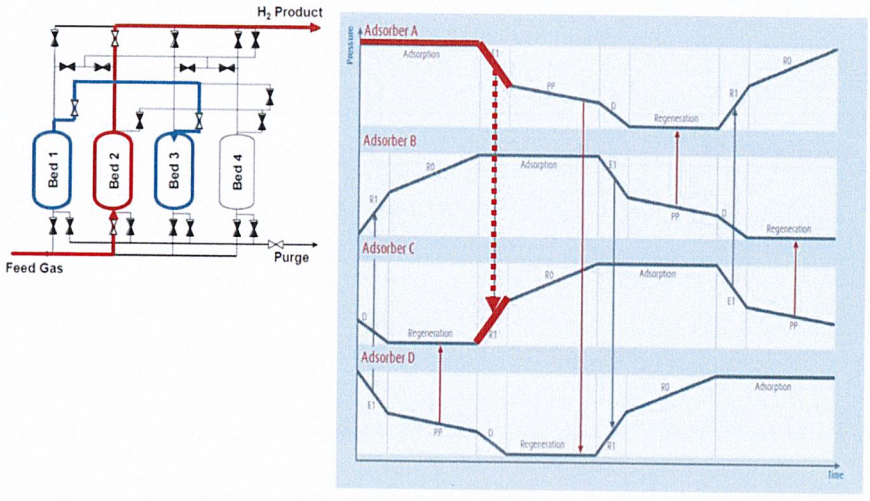

Figure 2.9 Pressure equalization step [The Linde Group, 2016]

2. Provide Purge (Step PP)

This is the final depressurization step in co- current direction providing pure hydrogen to purge or regenerate another adsorber.

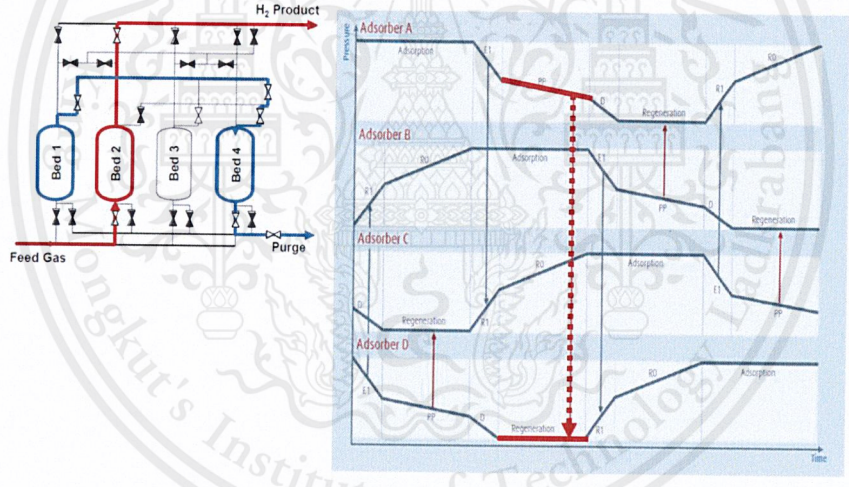

Figure 2.10 Provide purge step (Step PP) [The Linde Group, 2016]

3. Dump (Step D)

At a certain point of time, the remaining pressure must be released in counter-current direction to prevent break-through of impurities at the top of the adsorber. This is the first step of the regeneration phase when desorbed impurities leave the adsorber at the bottom and flow to the tail gas system of the PSA plant.

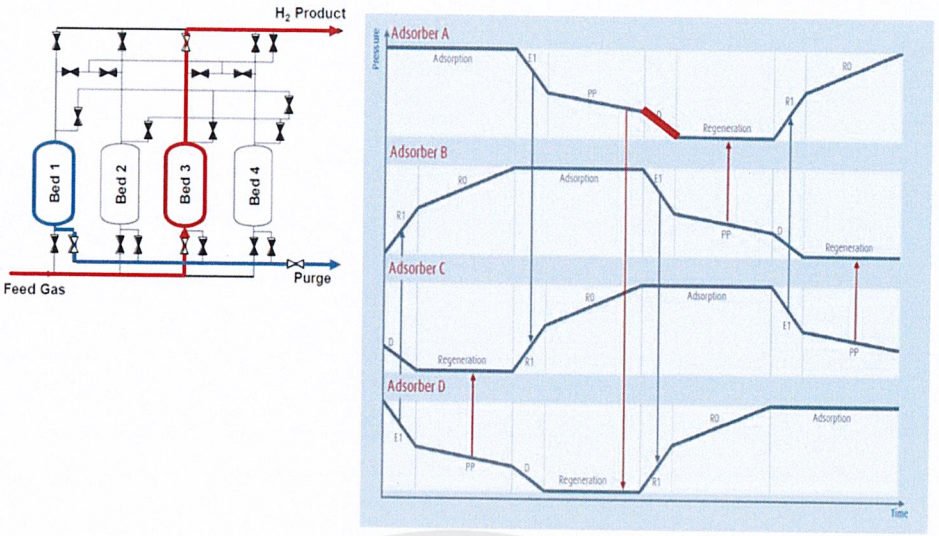

Figure 2.11 Dump step (Step D) [The Linde Group, 2016]

4. Purging (Regeneration)

Final desorption and regeneration is performed at the lowest pressure of the PSA sequence. Highly pure hydrogen obtained from an adsorber in the provide purge step, is used to purge the desorbed impurities into the tail gas system. The residual loading on the adsorbent material is reduced to a minimum to achieve high efficiency of the PSA cycle.

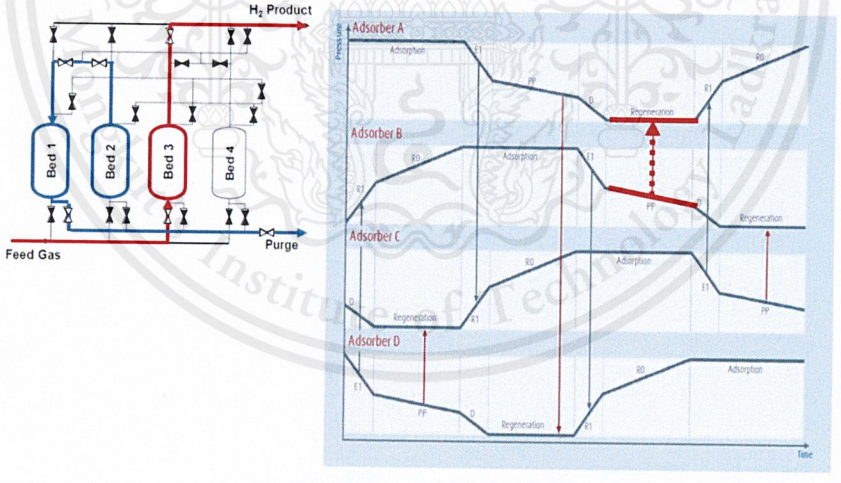

Figure 2.12 Purging step (Regeneration) [The Linde Group, 2016]

5. Repressurization (Step R1/R0)

Before restarting adsorption, the regenerated adsorber must be pressurized again. This is accomplished in the pressure equalization step by using pure hydrogen from adsorbers presently under depressurization. Since final adsorption

pressure cannot be reached with pressure equalization steps, repressurization to adsorption pressure is carried out with a split stream from the hydrogen product line. Having reached the required pressure level again, this regenerated adsorber takes over the task of adsorption from another vessel having just terminated its adsorption phase.

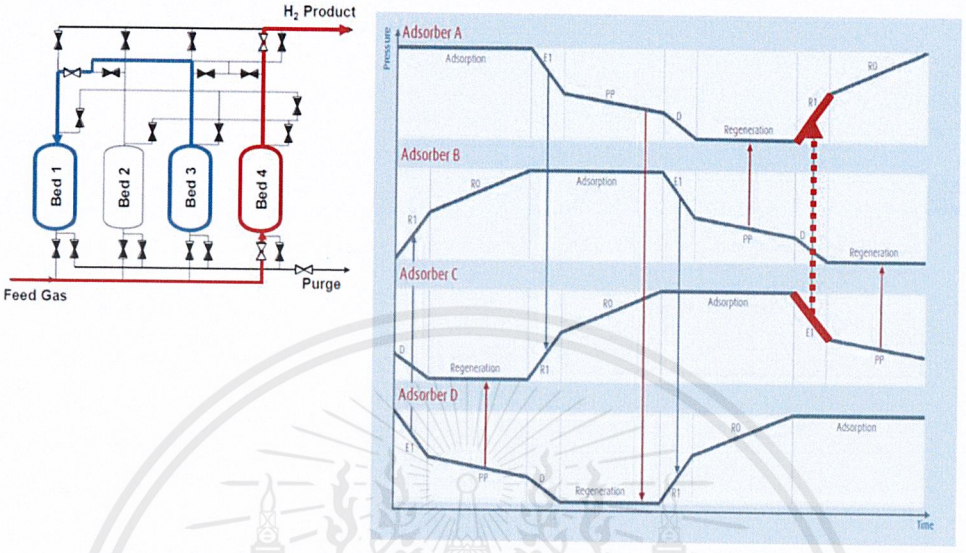

Figure 2.13 Repressurization step by equalization step from bed 3 (R1 step) [The Linde Group, 2016]

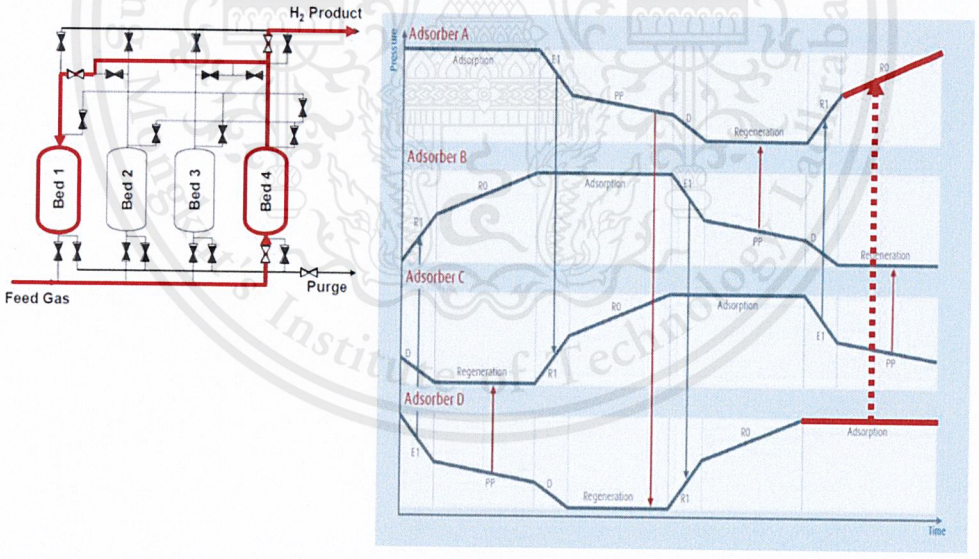

Figure 2.14 Repressurization step by adsorption step from bed 4 (R0 step) [The Linde Group, 2016]

2.2.1.5 Design of Fixed-Bed Adsorption Columns

Normally, fluid is passed through the packed bed at the constant flow rate. At the inlet to the bed, the solid is assumed to contain no solute at the start of the process. As the fluid first comes in contact with the inlet of the bed, most of the mass

transfer and adsorption takes place here. As the fluid passes through the bed, the concentration in this fluid drops very rapidly with distance in the bed and reaches zero well before the end of the bed is reached. The concentration profile at the start at time t_1 is shown in Figure 2.15a, where the concentration ratio c/c_0 is plotted versus bed height. The fluid concentration c_0 is the feed concentration and c is the fluid concentration at a point in the bed.

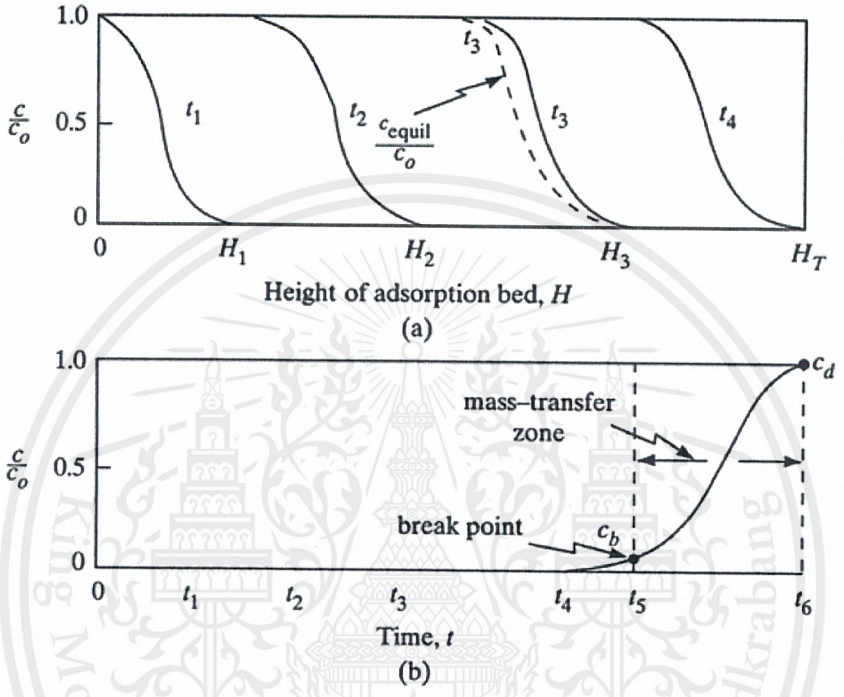

Figure 2.15 Concentration profiles for adsorption in a fixed bed: (a) profiles at various positions and times in the bed, (b) breakthrough concentration profile in the fluid at outlet of bed [Christie John Geankoplis, 2014]

After a short time, the solid near the entrance to the tower is almost saturated, and most of the mass transfer and adsorption now takes place at a point slightly farther from the inlet. At a later time t_2, the profile or mass-transfer zone where most of the concentration change takes place has moved farther down the bed. The concentration profiles shown are for the fluid phase. Concentration profiles for the concentration of adsorbates on the solid would be similar. The solid at the entrance would be nearly saturated, and this concentration would remain almost constant down to the mass-transfer zone, where it would drop off rapidly to almost zero. The dashed line for time t_3 shows the concentration in the fluid phase in equilibrium with the solid. The difference in concentrations is the driving force for mass transfer.

1. Breakthrough Concentration Curve

As seen in Figure 2.15a, the major part of the adsorption at any time takes place in a relatively narrow adsorption or mass-transfer zone. As the solution continues to flow, this mass-transfer zone, which is S-shaped, moves down the column. At a given time t_3 in Figure 2.15a, when almost half of the bed is saturated with solute, the outlet concentration is still approximately zero, as shown in Figure 2.15b. This outlet concentration remains near zero until the mass-transfer zone starts to reach the tower outlet at time t_4. Then the outlet concentration starts to rise, and at t_5 the outlet concentration has risen to c_b, which is called the break point.

After the break-point the concentration is rapidly rise to the point c_4 which is the end of the breakthrough curve. The break-point concentration represents the maximum that can be discarded and is often taken as 0.01 to 0.05 for c_b/c_0.

2. Capacity of Column and Scale-Up Design Method

Typically, adsorption process is designed by using results from experiments in laboratory scale. It is more accurate than predicted results from diffusion and mass transfer.

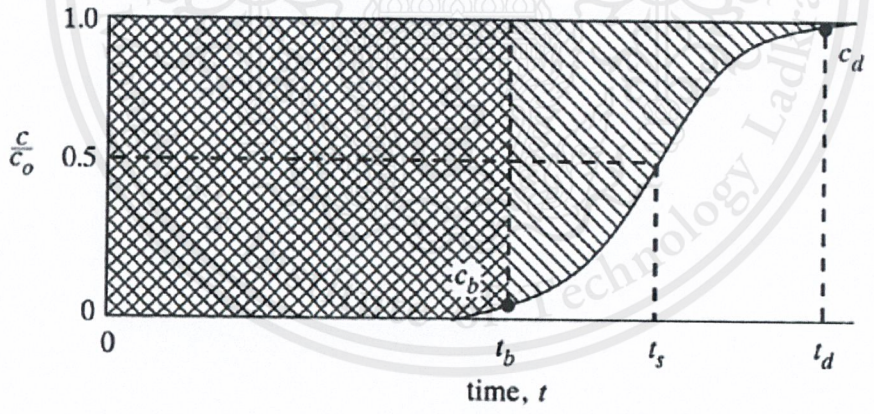

Figure 2.16 Determination of capacity of column from breakthrough curve [Christie John Geankoplis, 2014]

The total shaded area represents the total or stoichiometric capacity of the bed as shown in Figure 2.16. It is calculated by

$$t_t = \int_0^\infty (1 - \frac{c}{c_0})dt \qquad (2.1)$$

The usable capacity of the bed up to the break-point time t_b is the crosshatched area as shown in Figure 2.16. It is calculated by

$$t_u = \int_0^{t_b}(1 - \frac{c}{c_0})dt \quad (2.2)$$

The ratio of t_u/t_t is the fraction of the total bed capacity or length utilized up to the break point. Hence, for a total bed length of H_T, H_B is the length of bed used up to the break point.

$$H_B = \frac{t_u}{t_t} H_T \quad (2.3)$$

The length of unused bed H_{UNB} is then the unused fraction times the total length

$$H_{UNB} = (1 - \frac{t_u}{t_t})H_T \quad (2.4)$$

The H_{UNB} represents the mass transfer section which is depend on the fluid velocity. However, it is independent of total length of the column. Therefore, H_{UNB} is measured by using laboratory scale which is used small diameter laboratory column packed with designed adsorbent as same as in this project which find breakthrough curve from literature. It is shown later. Then the full-scale adsorber bed can be designed simply by first calculating the length of bed needed to achieve the required usable capacity, H_B, at the break point. The value of H_B is directly proportional to t_b. Then the length H_{UNB} of the mass-transfer section is simply added to the length H_B needed to obtain the total length, H_T

$$H_T = H_{UNB} + H_B \quad (2.5)$$

This is widely used for design method. It depends on the conditions in the laboratory column being similar to those for the full-scale unit. In the scale-up, not only may it be necessary to change the column height, but also the actual throughput of fluid might be different from that used in the experimental laboratory unit. Since the mass velocity in the bed must remain constant for scale-up, the diameter of the bed should be adjusted to keep it constant. However, it should be used spare are around 50% of used bed for design.

2.2.1.6 Pressure Swing Adsorption for Recovery Hydrogen

[Dong-Kyu Moon, 2016]

As discuss above, pressure swing adsorption for recovery hydrogen is designed from experimental in laboratory. From the "H_2 pressure swing adsorption for high pressure syngas from an integrated gasification combined cycle with a carbon capture process", is the literature of recovery hydrogen from syngas by using pressure swing adsorption technology. It uses H_2 -rich syngas at high pressure (30-35 bar) as feed. The feed contains five main components which are H_2:CO:N_2:CO_2:Ar =

88:3:6:2:1 mol%. To recover hydrogen, activated carbon is used for removal CO_2 and other impurities from hydrogen rich stream. However, N_2 and CO is hard to separate because they have low binding force as same as hydrogen. To remove N_2 and CO, zeolite LiX is used. So, the product is hydrogen at 99.77-99.95 % with 73-77.64 % recovery. This based on experiment operation at 293K. However, the efficiency of adsorbents is drop 20 to 30% as the temperature changed from 293 to 323 K. The characteristics of the adsorption bed, adsorbents and operating conditions in the experimental are shown in Table 2.2.

Table 2.2 Characteristics of the adsorption bed, adsorbents and operating conditions [Dong-Kyu Moon, 2016]

Adsorption bed		
Length, L (m)	1	
Adsorbent	**Zeolite LiX**	**Activated Carbon**
Type	Pellet	Cylindrical
Particle size, d_p (mm)	1.5-1.7	1.7-2.4
Particle density, ρ_p (g/cm^3)	1.050	0.750
Skeletal density, ρ_{sk} (g/cm^3)	2.000	1.850
Apparent density, ρ_b (g/cm^3)	0.7222	0.538
Bed porosity, $\varepsilon_b = (1 - \rho_b/\rho_p)$	0.312	0.283
Total porosity, $\varepsilon_t = (1 - \rho_b/\rho_{sk})$	0.639	0.709
Heat capacity, C_{ps} (J/kg K)	1070	1570
Pore volume (cm^3/g)	0.39	0.46
Total surface area (m^2/g)	664.7	1306.4
Operating Condition		
Flow rate, Q_{Feed} (SLPM)*	5	
Temperature, T_{Feed} (^{O}C)	35	
Adsorption Pressure, P_{AD} (bar)	35	
Desorption Pressure, P_{PG} (bar)	1.1	

Hydrogen Recovery Experimental

This experiment uses 2 bed. In the pressure swing adsorption operation that employs layers beds, the zeolite layer should be protected from CO_2 propagation because of

difficult regeneration and the high heat of adsorption. In the study, the adsorption bed packed with zeolite LiX followed by activated carbon in the layered bed (bottom (AC) and top (zeolite LiX)) is recommended for enhancing the separation efficiency in the ratio of AC:LiX = 8:2. Activated carbon is expected to remove CO_2 and a zeolite with an enhanced capacity for CO and N_2 is ultimately employed. Because the accumulated CO_2 on zeolite LiX will result in a detrimental effect on the pressure swing adsorption performance. The results of the breakthrough experiment and simulation at 35 bar and 5 LSTP/min conditions are shown in Figure 2.17.

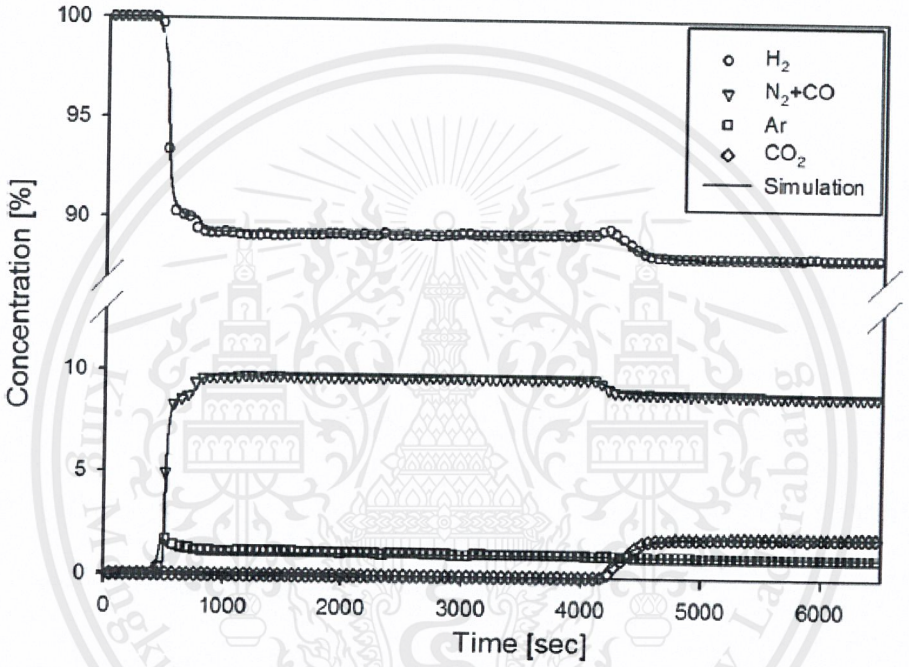

Figure 2.17 Breakthrough curves in the activated carbon bed and the zeolite LiX bed at the ratio of AC:LiX = 8:2 (At 35 bar and 5 LSTP/min) [Dong-Kyu Moon, 2016]

The breakthrough time of N_2 + CO in the activated carbon bed was observed to be close to 475 second which accompanied the decrease in hydrogen concentration.

2.2.2 Membrane Separation [Logan Scott McLeod, 2008]

Membranes have been utilized for hydrogen separation/purification since the early 1960's. In the mid-1970's the first successful polymer hydrogen membrane was developed by DuPont using small-diameter, hollow fibers.

Membrane separation is based on the difference between in permeation rates (hydrogen and impurities). Permeation involves two sequential mechanisms: the component of gas phase must first dissolve into the membrane and then diffuse through

to the permeate side. Different components have different solubility and permeation rates. Solubility depends on the chemical composition of the membrane and diffusion on the structure of the membrane. Components with higher permeability, such as hydrogen, dissolve in to the polymer membrane on the high pressure side to the low pressure side. However, components with lower permeability, are retained on the high pressure side because of the depletion of components with high permeability. High permeation rates are due to high solubilities, high diffusivities, or both. The driving force is the difference in partial pressure, with the highest driving force giving the highest recovery. Economically, this is a potential drawback of membrane separation compared with PSA which need a compressor to supplied at elevated pressure.

Permeability is defined as flux of gas species with the membrane thickness divided by the applied partial pressure difference across the membrane. Permeability is useful for comparison between different membrane materials under different test conditions as the effects of membrane thickness. Selectivity is defined as the ratio of permeabilities between two different species. Materials with both high permeability and high selectivity for the gas species of interest are desirable. Higher permeability reduces the amount of membrane area required for a given application and therefore reduces cost. Higher selectivity increases the purity of the product gas.

In addition to permeability and selectivity, membrane strength, durability, operating environment (compatible gas species), operating temperature range, and susceptibility to fouling are all important factors to be considered in choosing a membrane for a given application.

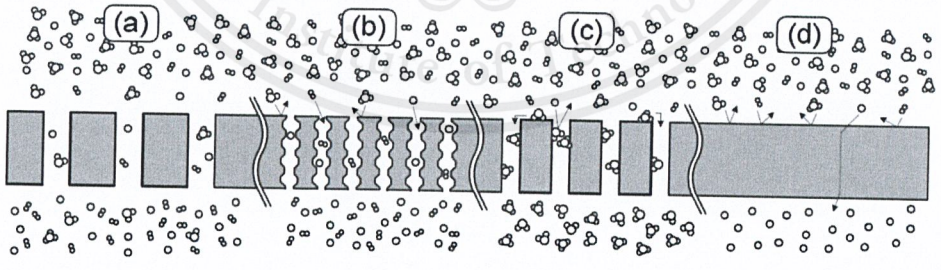

Figure 2.18 Transport mechanisms for membrane-based gas separation: (a) Knudsen diffusion, (b) molecular sieving, (c) surface diffusion and (d) solution-diffusion [Logan Scott McLeod, 2008]

Membrane, gas separation is divided following the transport mechanisms (Figure 2.18): Knudsen diffusion, surface diffusion, molecular sieving, and solution-diffusion. Knudsen diffusion is characterized by pore dimensions (Figure 2.18(a))

which transport is occurred by the collisions of the substance molecule. The Knudsen diffusion coefficient can be derived from kinetic theory and proportional to the velocity of a gas species. Different gas species at the same temperature must have equivalent energy and since this energy is largely kinetic, heavier gas molecules have a lower velocity. In fact, the ratio of their velocities, and therefore their relative Knudsen diffusion rate, is proportional to the inverse ratio of the gas molecular weights to the one-half power. Molecular sieving membranes are made either of rigid crystalline structures with well-defined pore size or of tightly-packed amorphous materials with a narrow distribution of pore sizes. In either case, pore size must be below ~10 angstroms (Å) for molecular sieving to occur. These pores physically exclude gas molecules of larger dimensions and can therefore potentially provide excellent selectivity (Figure 2.18(b)). Surface diffusion involves adsorption of the gas species on the membrane surface, followed by diffusion along the surface through pores or through defects/grain boundaries from one surface to the other (Figure 2.18(c)). This method has the advantage that the adsorbing species and the selectively permeates, can be isolated based on specific surface chemistry. Typically, this approach allows larger gas species to permeate more quickly. The final mechanism is solution-diffusion (Figure 2.18(d)). This mechanism is absorption of the gas species into the membrane on the upstream surface. Once absorbed, the gas must diffuse through the membrane and then desorb from the downstream surface. The permeation rate for this process is controlled by both the solubility of the gas species in the membrane and the diffusion coefficient of the absorbed species through the membrane.

In addition to the mechanism employed for separation, it is often useful to categorize membranes based on the materials used. Hydrogen membranes which is used for recovery hydrogen can be broadly categorized into polymer and metallic membrane. This classification allows a more direct comparison of membrane permeability, selectivity, operating conditions and cost.

2.2.2.1 Polymeric Membrane

Hydrogen recovery using polymeric membrane is based on differences between permeability of feed stream components. Gases with high permeability pass through the membrane faster than the other gases. In this process, hydrogen is more permeable than other impurities and passes through the membrane faster. So, the product stream will be enriched in hydrogen. Higher hydrogen permeability leads to

better separation and lesser required energy for the process. Product purity is strongly influenced by membrane selectivity and the pressure difference between feed and permeate. To enhance hydrogen recovery, membrane area should be increased. Another way to reach higher recovery is increasing pressure difference between the two sides of the membrane, which can impose additional costs in order to raise the pressure of feed or product stream. The membranes usually need to be replaced every 4 to 5 years due to loss of performance.

2.2.2.2 Metallic Membranes

In 1962 the National Cylinder Gas division of the Chemetron Co. constructed a commercial-scale plant capable of producing 115,000 ft^3/day of hydrogen with less than 0.1 parts per million (PPM) of impurities. This plant utilized thin Pd-alloy tubes and was the first commercial implementation of a hydrogen membrane. Interestingly, it had been almost 100 years since the original discovery in 1866 that certain metals were highly permeable to hydrogen. The long delay was primarily due to the fact that most metals that are permeable to hydrogen also form a metal hydride with different physical characteristics than the metal. Transition into a metal hydride causes membrane failure and is typically labeled hydrogen embrittlement. Metal membranes were able to be utilized commercially after the discovery by Hunter in 1960 that alloying palladium with silver eliminated the embrittlement and failure issues that plagued pure Pd and other metals. The low hydrogen flux achievable with these relatively thick-walled early Pd-alloy tubes, coupled with the high cost of Pd, made this approach to hydrogen purification uneconomical and these plants were not widely adopted. However, small-scale hydrogen purification systems based on this technology where ultra-high purity is required, such as laboratory research and semiconductor manufacture, are in use and commercially available today.

Hydrogen permeation through metals occurs via the solution-diffusion mechanism. Due to the fact that hydrogen adsorption onto the metal surface is dissociative, this process is sometimes called reactive or catalytic solution-diffusion. Palladium-alloys, especially with copper and silver, are the primary metals utilized due to their high surface reactivity for hydrogen dissociation, resistance to embrittlement, and high hydrogen permeability. The permeability of Pd-alloys by hydrogen is the highest of all membrane materials. Pd-alloys are typically operated at temperatures from 300-600 °C and exhibit good mechanical properties. Although Pd-alloys have

higher permeability than other membrane materials the achievable flux is often limited by the thickness of the metal films. While other materials are consistently fabricated with a thickness less than 100 nm, defect-free metal membranes with a thickness of less than a few microns have been elusive. In addition, metal membranes are susceptible to fouling/poisoning of the surface from gases such as H_2S and HCl and the high cost of Pd makes these membranes expensive.

The percent purity and percent recovery of the metallic and polymer membrane are compared in Figure 19.

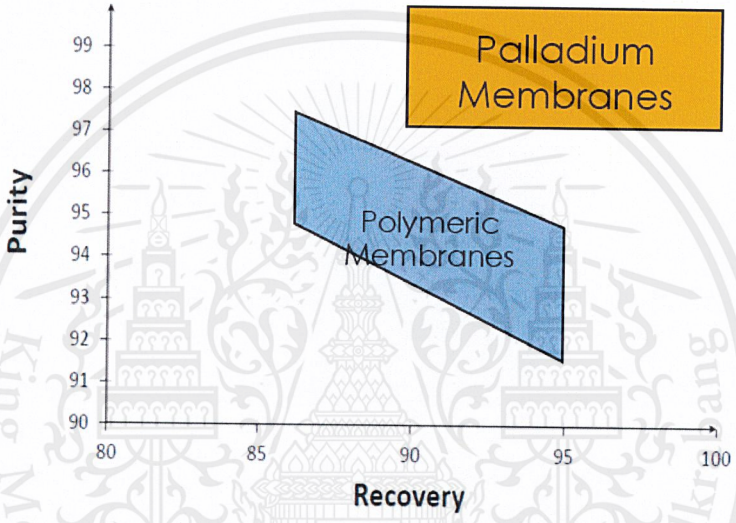

Figure 2.19 Percent purity and recovery of the metallic and polymer membrane [Gazzani Matteo, 2015]

However, the common disadvantages of membranes are

1. The hydrogen product stream is produced at pressures much lower than the feed pressure need recompression.
2. Changes in feed composition will have a large effect on product purity. Membranes have no moving parts and are reliable.

2.2.3 Cryogenic Separation [Ali Muvechain and Majid Pakizeh, 2013]

Cryogenic separation unit are based on the difference in volatility (boiling point temperature) of the feed components. Hydrogen has a high relative volatility compared with other impurities. In this process, amount of feed impurities is condensed by cooling system. This process is typically applied for separation of hydrogen-hydrocarbon. Feed contain impurities will pass to cooling system. Two-phases stream

is sent to the separator for separate product (hydrogen) at the overhead and impurities at the bottom zone (Figure 2.20). The process will separate impurities in cycle depend on desired hydrogen purity. The hydrogen purity can reach to 99% purity. Furthermore, impurities such as methane or water can reuse from this process.

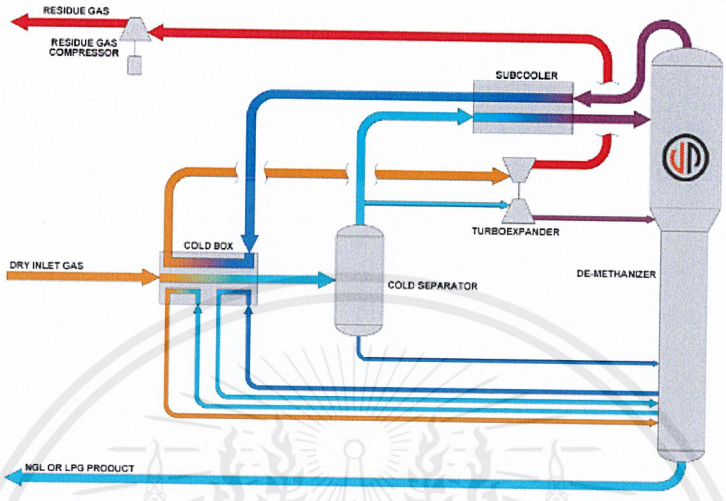

Figure 2.20 Cryogenic process [Joule processing, 2016]

Cryogenic process is the cost intensive and in processing varying feed composition has less flexibility and sometimes requires supplemental refrigeration and is considered less reliable than PSA or a membrane and the feed needs pretreatment. Due to disadvantages of cryogenic process for hydrogen purification, typically not used in PTA process and therefore it was not considered in this study.

2.3 Pre-Treatment Units

Generally, the impurities from CTA are not only 4-CBA and p-TA but also water, benzoic acid, carbon monoxide, carbon dioxide, nitrogen and micro powder terephthalic acid. However, the main impurities are water and benzoic acid. Water is in a large value around 99% and benzoic acid is the organic compound which effect to HRU. So, there are the main impurities that are the reason to require pre-treatment process, condenser and scrubber, respectively.

2.3.1 Heat Exchanger and Condenser [R.K. Sinnott, 2005]

Condenser is designed for remove water by using circulated cooling water. However, not only water is condensed but also TA, *p*-TA and 4-CBA. All of these impurities will dissolved and remove when water is condensed by condenser. So, the condenser or heat exchanger are designed.

The principal types of heat exchanger used in the chemical process and allied industries are

1. Double-pipe exchanger: the simplest type, used for cooling and heating
2. Shell and tube exchangers: used for all applications
3. Plate and frame exchangers (plate heat exchangers): used for heating and cooling
4. Plate-fin exchangers
5. Spiral heat exchangers
6. Air cooled: used for coolers and condensers
7. Direct contact: used for cooling and quenching
8. Fired heaters
9. Agitated vessels

The word *exchanger* really applies to all types of equipment in which heat is exchanged but is often used specifically to denote equipment in which heat is exchanged between two process streams. Exchangers in which a process fluid is heated or cooled by a plant service stream are referred to as heaters and coolers. If the process stream is vaporized, the exchanger is called a *vaporizer* if the stream is essentially completely vaporized, a reboiler if associated with a distillation column, and an evaporator if used to concentrate a solution. The terms fired exchanger and fired heater are used for exchangers heated by combustion gases, such as boilers; other exchangers are referred to as unfired exchangers.

2.3.1.1 Basic Design Procedure and Theory

The general equation for heat transfer across a surface is

$$Q = UA\Delta T_{lm} \tag{2.6}$$

The prime objective in the design of an exchanger is to determine the surface area required for the specified duty (rate of heat transfer) using the temperature differences available.

The overall coefficient is the reciprocal of the overall resistance to heat transfer, which is the sum of several individual resistances. For heat exchange across a typical heat exchanger tube, the relationship between the overall coefficient and the individual coefficients, which are the reciprocals of the individual resistances, is given by

$$\frac{1}{U} = \frac{1}{h_o} + \frac{1}{f_o} + \frac{d_o \ln(\frac{d_o}{d_i})}{2k_w} + \frac{d_o}{d_i} \times \frac{1}{f_i} + \frac{d_o}{d_i} \times \frac{1}{h_i} \quad (2.7)$$

The magnitude of the individual coefficients will depend on the nature of the heat transfer process (conduction, convection, condensation, boiling, or radiation), on the physical properties of the fluids, on the fluid flow rates, and on the physical arrangement of the heat transfer surface. As the physical layout of the exchanger cannot be determined until the area is known, the design of an exchanger is of necessity a trial and error procedure. The steps in a typical design procedure are as follows:

1. Define the duty: heat transfer rate, fluid flow rates, temperatures.
2. Collect together the fluid physical properties required: density, viscosity, thermal conductivity.
3. Decide on the type of exchanger to be used.
4. Select a trial value for the overall coefficient, U.
5. Calculate the mean temperature difference, ΔT_{lm}.
6. Calculate the area required from equation 2.6.
7. Decide the exchanger layout.
8. Calculate the individual coefficients.
9. Calculate the overall coefficient and compare with the trial value. If the calculated value differs significantly from the estimated value, substitute the calculation for the estimated value and return to step 6.
10. Calculate the exchanger pressure drop; if unsatisfactory, return to steps 7 or 4 or 3, in that order of preference.
11. Optimize the design: repeat steps 4 to 10, as necessary, to determine the cheapest exchanger that will satisfy the duty.

2.3.1.2 Overall Heat Transfer Coefficient

Typical values of the overall heat transfer coefficient for various types of heat exchanger are given in Table 2.3.

Table 2.3 Typical overall coefficients [R.K. Sinnott, 2005]

Shell and Tube Exchangers		
Hot Fluid	**Cold Fluid**	***U* (W/m²°C)**
Heat exchangers		
Water	Water	800–1500
Organic solvents	Organic solvents	100–300
Light oils	Light oils	100–400
Heavy oils	Heavy oils	50–300
Gases	Gases	10–50
Coolers		
Organic solvents	Water	250–750
Light oils	Water	350–900
Heavy oils	Water	60–300
Gases	Water	20–300
Organic solvents	Brine	150–500
Water	Brine	600–1200
Gases	Brine	15–250
Heaters		
Steam	Water	1500–4000
Steam	Organic solvents	500–1000
Steam	Light oils	300–900
Steam	Heavy oils	60–450
Steam	Gases	30–300
Dowtherm	Heavy oils	50–300
Dowtherm	Gases	20–200
Flue gases	Steam	30–100
Flue	Hydrocarbon vapors	30–100
Condensers		
Aqueous vapors	Water	1000–1500
Organic vapors	Water	700–1000
Organics (some noncondensables)	Water	500–700
Vacuum condensers	Water	200–500
Vaporizers		
Steam	Aqueous solutions	1000–1500
Steam	Light organics	900–1200
Steam	Heavy organics	600–900

The values given in Table 2.3 can be used for the preliminary sizing of equipment for process evaluation and as trial values for starting a detailed thermal design.

2.3.1.3 Fouling factors (Dirt factors)

Most process and service fluids will foul the heat transfer surfaces in an exchanger to a greater or lesser extent. The deposited material will normally have a relatively low thermal conductivity and will reduce the overall coefficient. It is therefore necessary to oversize an exchanger to allow for the reduction in performance during operation. The effect of fouling is allowed for in design by including the inside and outside fouling coefficients in equation 2.7. Fouling factors are usually quoted as heat transfer resistances rather than coefficients. They are difficult to predict and are

usually based on past experience. Typical values for the fouling coefficients and factors for common process and service fluids are given in Table 2.4. These values are for shell and tube exchangers with plain (not finned) tubes.

Table 2.4 Fouling factors (coefficients), typical values [R.K. Sinnott, 2005]

Fluid	Coefficient ($W/m^2°C$)	Factor (resistance) ($m^2°C/W$)
River water	3000–12,000	0.0003–0.0001
Sea water	1000–3000	0.001–0.0003
Cooling water (towers)	3000–6000	0.0003–0.00017
Towns water (soft)	3000–5000	0.0003–0.0002
Towns water (hard)	1000–2000	0.001–0.0005
Steam condensate	1500–5000	0.00067–0.0002
Steam (oil free)	4000–10,000	0.0025–0.0001
Steam (oil traces)	2000–5000	0.0005–0.0002
Refrigerated brine	3000–5000	0.0003–0.0002
Air and industrial gases	5000–10,000	0.0002–0.0001
Flue gases	2000–5000	0.0005–0.0002
Organic vapours	5000	0.0002
Organic liquids	5000	0.0002
Light hydrocarbons	5000	0.0002
Heavy hydrocarbons	2000	0.0005
Boiling organics	2500	0.0004
Condensing organics	5000	0.0002
Heat transfer fluids	5000	0.0002
Aqueous salt solutions	3000–5000	0.0003–0.0002

2.3.1.4 Shell and Tube Exchangers: Construction Details

The shell and tube exchanger is by far the most common type of heat transfer equipment used in the chemical and allied industries. The advantages of this type are as follows:

1. The configuration gives a large surface area in a small volume;
2. Good mechanical layout: a good shape for pressure operation;
3. Uses well-established fabrication techniques;
4. Can be constructed from a wide range of materials;
5. Easily cleaned;
6. Well-established design procedures.

Essentially, a shell and tube exchanger consists of a bundle of tubes enclosed in a cylindrical shell. The ends of the tubes are fitted into tube sheets, which separate the shell-side and tube-side fluids. Baffles are provided in the shell to direct the fluid flow and support the tubes. The assembly of baffles and tubes is held together by support rods and spacers, as shown in Figure 2.21.

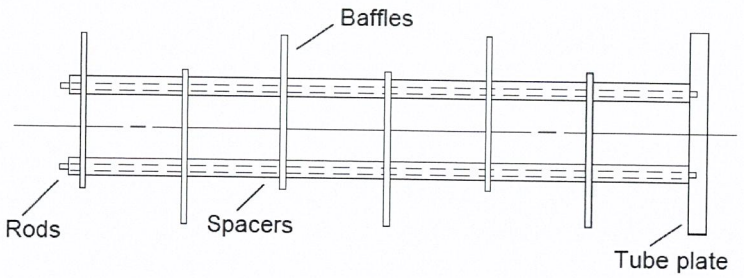

Figure 2.21 Baffle spacers and tie rods [R.K. Sinnott, 2005]

2.3.1.5 Exchanger Types

The principal types of shell and tube exchanger are shown in Figures 2.22 to 2.24.

Nomenclature

1. Shell
2. Shell cover
3. Floating-head cover
4. Floating-tube plate
5. Clamp ring
6. Fixed-tube sheet (tube plate)
7. Channel (end-box or header)
8. Channel cover
9. Branch (nozzle)
10. Tie rod and spacer
11. Cross baffle or tube-support plate
12. Impingement baffle
13. Longitudinal baffle
14. Support bracket
15. Floating-head support
16. Weir
17. Split ring
18. Tube
19. Tube bundle
20. Pass partition
21. Floating-head gland (packed gland
22. Floating-head gland ring
23. Vent connection
24. Drain connection
25. Test connection
26. Expansion bellows
27. Lifting Ring

The simplest and cheapest type of shell and tube exchanger is the fixed tube sheet design shown in Figure 2.24 (TEMA type BEM). The main disadvantages of this type are that the tube bundle cannot be removed for cleaning, and there is no provision for differential expansion of the shell and tubes. As the shell and tubes will be at different temperatures and may be of different materials, the differential expansion can be considerable. Some provision for expansion can be made by including an expansion loop in the shell (shown dotted on Figure 2.24), but their use is limited to

low shell pressure, up to about 8 bar. In the other types, only one end of the tubes is fixed, and the bundle can expand freely.

The U-tube (U-bundle) type, shown in Figure 2.22, requires only one tube sheet and is cheaper than the floating-head types. It is widely used but is limited in use to relatively clean fluids, as the tubes and bundle are difficult to clean. It is also more difficult to replace a tube in this type. Exchangers with an internal floating head, as shown in Figures 2.23 are more versatile than fixed-head and U-tube exchangers. They are suitable for high temperature differentials and, as the tubes can be rodded from end to end and the bundle removed, are easier to clean and can be used for fouling liquids. A disadvantage of the pull-through design, shown in Figure 2.23, is that the clearance between the outermost tubes in the bundle and the shell must be made greater than in the fixed and U-tube designs to accommodate the floating-head flange, allowing fluid to bypass the tubes.

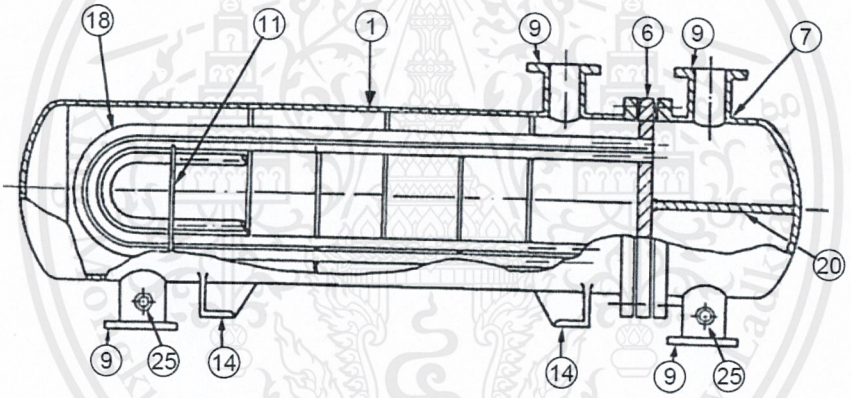

Figure 2.22 U-tube heat exchanger [R.K. Sinnott, 2005]

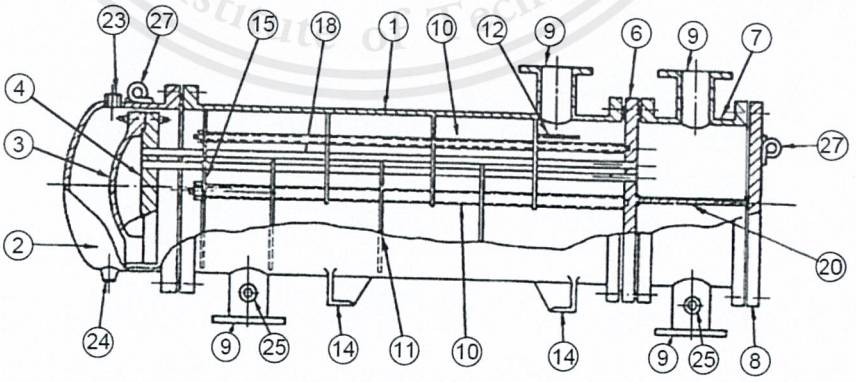

Figure 2.23 Internal floating head without clamp ring [R.K. Sinnott, 2005]

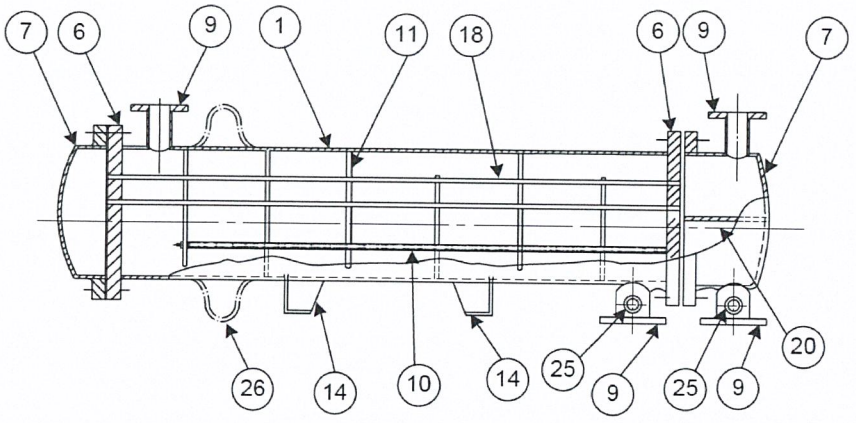

Figure 2.24 Fixed-tube plate heat exchanger [R.K. Sinnott, 2005]

2.3.1.6 Tubes

Normally, Tube diameter is used in range of 16 – 55 mm which prefer smaller diameter for high duty and cheaper for the exchanger. However, larger tubes are easier to clean by mechanical methods and would be selected for heavily fouling fluids. The optimum tube length to shell diameter will usually fall within the rage of 5 to 10 m or by using the old design.

2.3.1.6.1 Tube Arrangements

The tubes in an exchanger are usually arranged in an equilateral triangular, square or rotated square pattern (Figure 2.25).

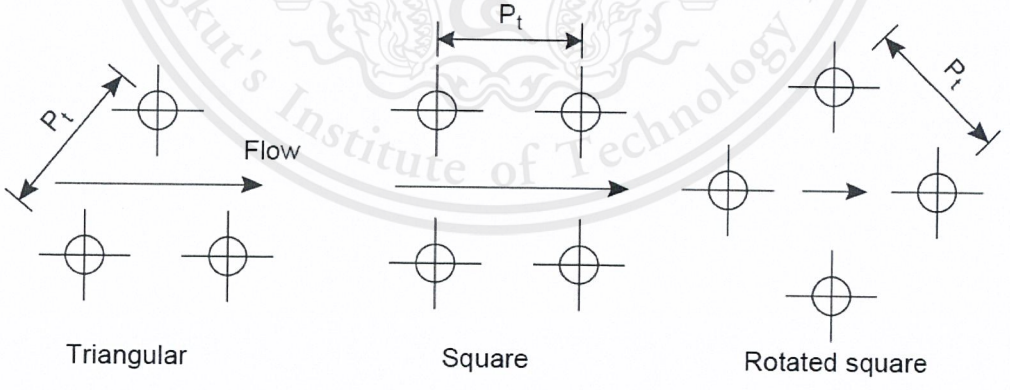

Figure 2.25 Tube patterns [R.K. Sinnott, 2005]

The triangular and rotated square patterns give higher heat transfer rates, but at the expense of a higher pressure drop than the square pattern. A square or rotated square arrangement is used for heavily fouling fluids, where it is necessary to mechanically clean the outside of the tubes. The recommended tube pitch (distance between tube centers) is 1.25 times the tube outside diameter, and this will normally be

used unless process requirements dictate otherwise. For the tube-side pass is selected to give the required tube-side design velocity around 1-2 m/s for the liquid.

2.3.1.7 Shells

The shell diameter must be selected to give as close a fit to the tube bundle as is practical, to reduce bypassing round the outside of the bundle. The clearance required between the outermost tubes in the bundle and the shell inside diameter will depend on the type of exchanger and the manufacturing tolerances; typical values are given in Figure 2.26.

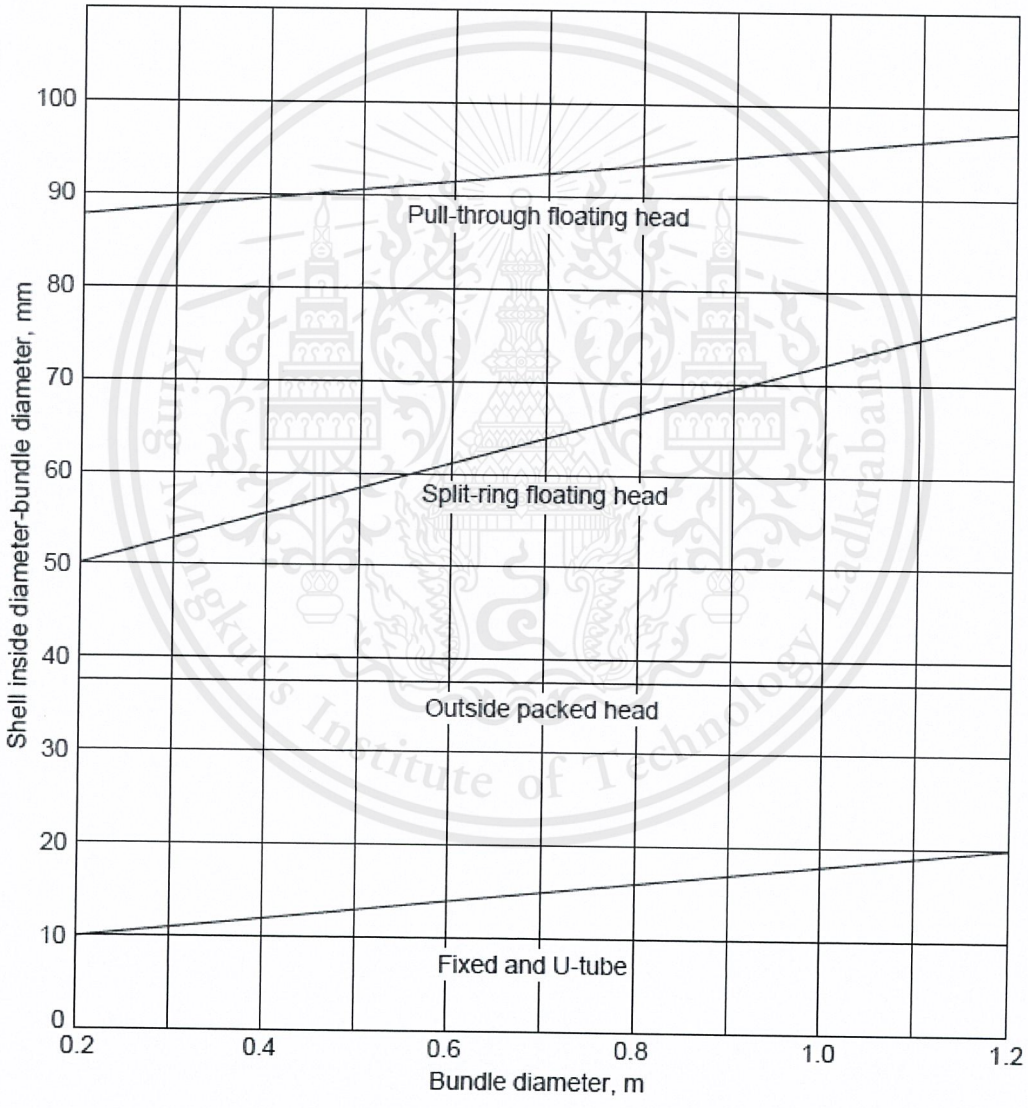

Figure 2.26 Shell-bundle clearance [R.K. Sinnott, 2005]

The bundle diameter D_b is calculated by

$$D_b = d_o\left(\frac{N_t}{K_1}\right)^{\frac{1}{n}} \tag{2.8}$$

The number of tubes in the center row, the row at the shell equator is calculated by

$$\text{Tube in center row} = D_b/P_t \tag{2.9}$$

Table 2.5 Constants value for bundle diameter calculation [R.K. Sinnott, 2005]

Triangular Pitch, $p_t = 1.25d_o$					
No. passes	1	2	4	6	8
K_1	0.319	0.249	0.175	0.0743	0.0365
$>n_1$	2.142	2.207	2.285	2.499	2.675
Square Pitch, $p_t = 1.25d_o$					
No. passes	1	2	4	6	8
K_1	0.215	0.156	0.158	0.0402	0.0331
n_1	2.207	2.291	2.263	2.617	2.643

2.3.1.8 Mean Temperature Difference (Temperature Driving Force)

Log mean temperature is the temperature difference in function of logarithm between hot fluid temperature inlet, hot fluid temperature outlet, cold fluid temperature inlet and cold fluid temperature outlet. Log mean temperature difference is calculated by

$$\Delta T_{lm} = \frac{(T_1-t_2)-(T_2-t_1)}{\ln((T_1-t_2)/(T_2-t_1))} \tag{2.10}$$

However, design of shell and tube exchanger is usually estimate the "true temperature difference" from the logarithmic mean temperature by using a correction factor

$$\Delta T_{lm} = F_t \Delta T_{lm} \tag{2.11}$$

The correction factor is a function of the shell and tube fluid temperatures, and the number of tube and shell passes. It is normally correlated as a function of two dimensionless temperature ratios which shown below

$$R = \frac{T_1-T_2}{t_2-t_1} \tag{2.12}$$

and

$$S = \frac{t_2-t_1}{T_1-t_2} \tag{2.13}$$

R is equal to the shell side fluid flow-rate times the fluid mean specific heat divided by the tube side fluid flow rate times the tube side fluid specific heat

S is a measure of the temperature efficiency of the exchanger

The correction factor is found from the Figure 2.27 as plot by S and R to find correction factor.

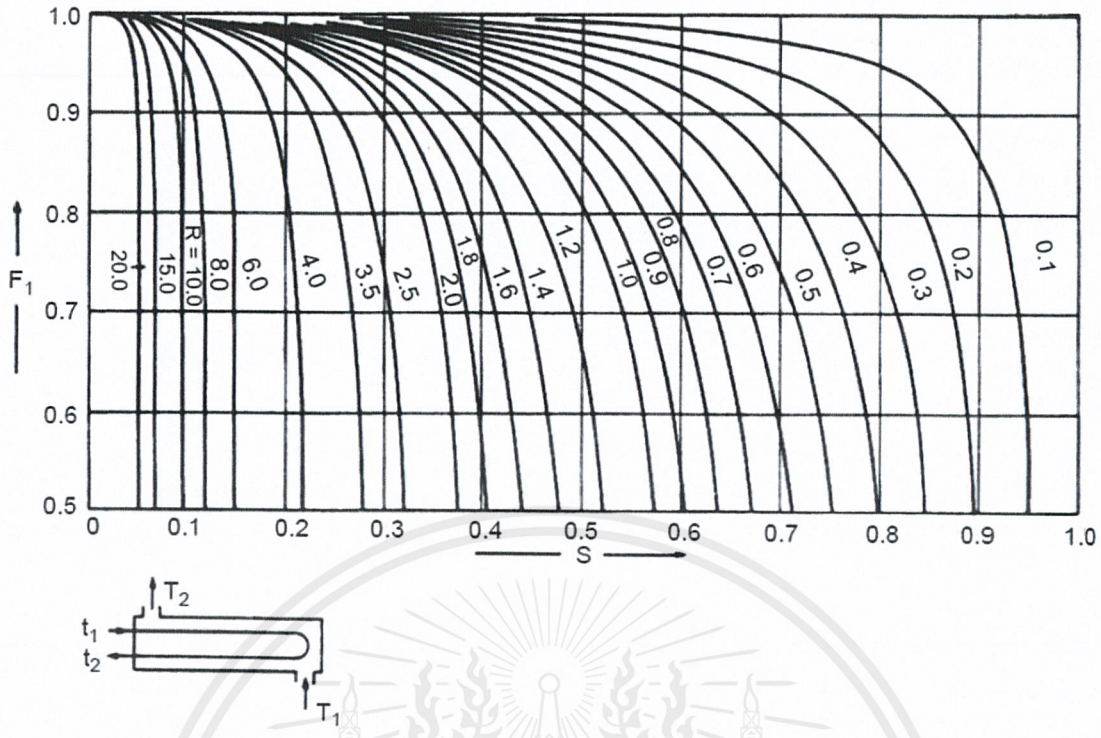

Figure 2.27 Temperature correction factor: one shell pass; two or more even tube passes [R.K. Sinnott, 2005]

2.3.1.9 Tube Side Heat Transfer Coefficient and Pressure Drop

Tube side heat transfer coefficient

Generally, heat transfer coefficient inside pipe for turbulent flow is calculated by

$$Nu = CRe^{a}Pr^{B}(\frac{\mu}{\mu_w})^{c} \tag{2.14}$$

For more accurate estimate, the equations which developed specifically for water are used (The equation has been adapted from data given by Eagle and Ferguson)

$$h_i = \frac{4200(1.35+0.02t)u_t^{0.8}}{d_i^{0.2}} \tag{2.15}$$

Tube side pressure drop

The pressure drop in tube is occurred from friction loss in tube. There are calculated by

$$\Delta P_s = N_p\left(8\times j_f\times\frac{L}{l_B}+2.5\right)\times\frac{\rho u_t^2}{2} \tag{2.16}$$

Values of j_f for heat exchanger tubes can be obtained from Figure 2.28.

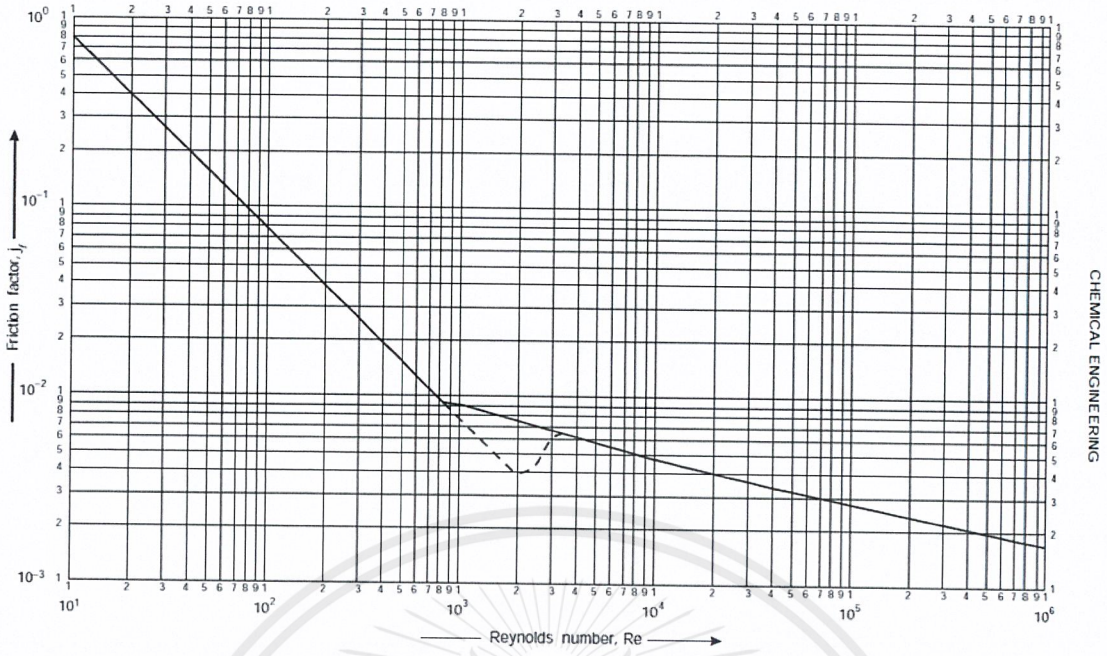

Figure 2.28 Tube-side friction factors [R.K. Sinnott, 2005]

2.3.1.10 Shell Side Heat Transfer and Pressure Drop

To preliminary design calculations, Kern's method is used because it is simple to apply and accurate enough.

Kern's method

This method was based on experimental work on commercial exchangers with standard tolerances and will give a reasonably satisfactory prediction of the heat transfer coefficient for standard designs. The prediction of pressure drop is less satisfactory, as pressure drop is more affected by leakage and bypassing than heat transfer. The shell-side heat transfer and friction factors are correlated in a similar manner to those for tube-side flow by using a hypothetical shell velocity and shell diameter. As the cross-sectional area for flow will vary across the shell diameter, the linear and mass velocities are based on the maximum area for cross-flow: that at the shell equator. The shell equivalent diameter is calculated using the flow area between the tubes taken in the axial direction (parallel to the tubes) and the wetted perimeter of the tubes; see Figure 2.29.

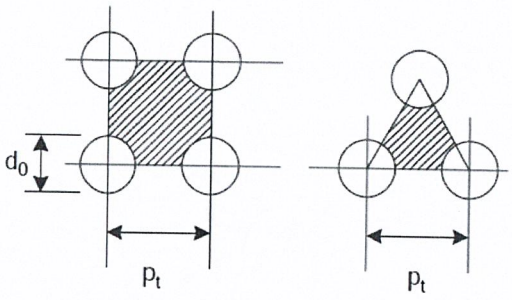

Figure 2.29 Equivalent diameter, cross-sectional area and wetted perimeters [R.K. Sinnott, 2005]

Shell side j_h and j_f factors for use in this method are given in Figure 2.30 and 2.31.

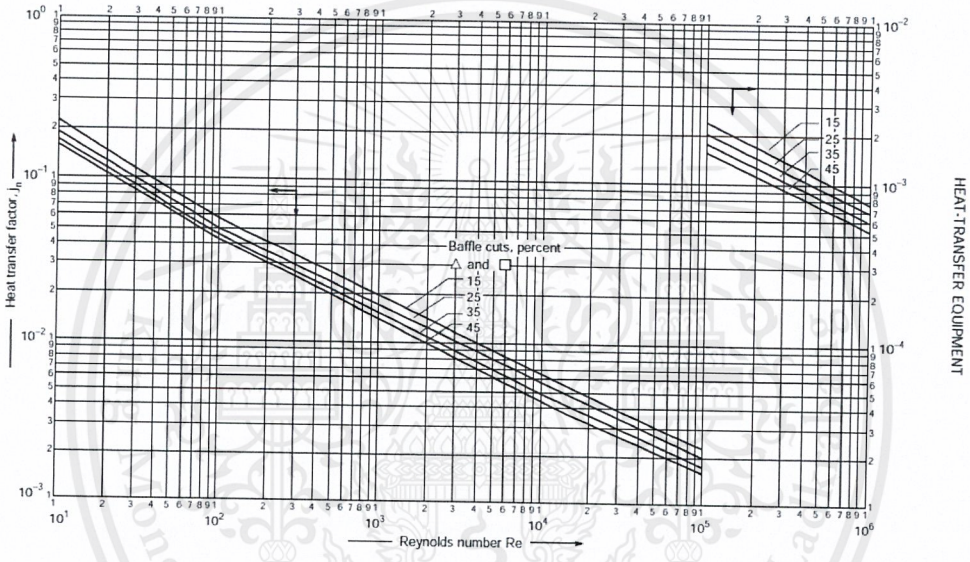

Figure 2.30 Shell side heat transfer factors, segmental baffles [R.K. Sinnott, 2005]

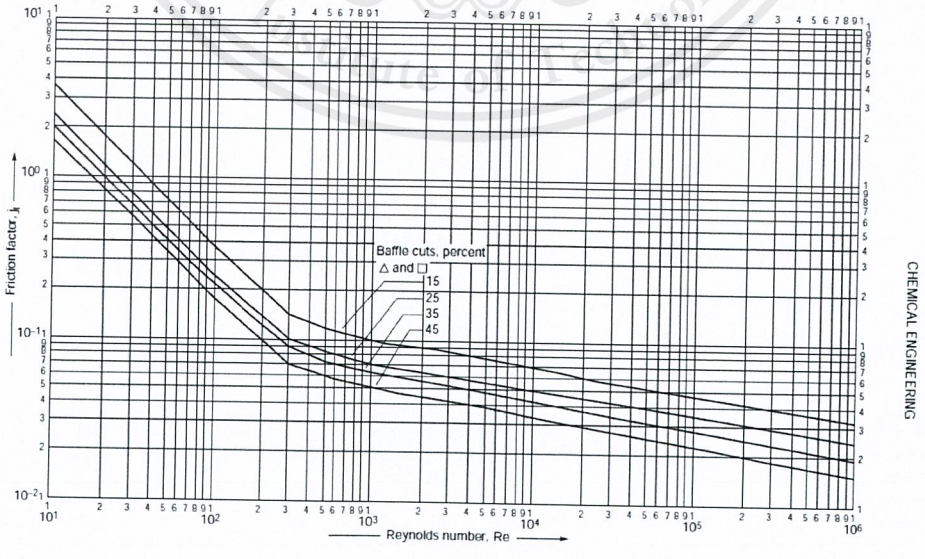

Figure 2.31 Shell side friction factors, segmental baffles [R.K. Sinnott, 2005]

The calculation design for shell side heat transfer coefficient and pressure drop are followed procedure as shown below

Procedure

1. Calculate the area for cross flow A_s

$$A_s = \frac{(p_t - d_o)}{p_t} D_s l_B \tag{2.17}$$

The term $\frac{(p_t - d_o)}{p_t}$ is the raio of the clearance between tubes and the total distance between tube centers.

2. Calculate the shell side mass velocity G_s and the linear velocity u_s

$$G_s = \frac{W_s}{A_s} \tag{2.18}$$

$$u_s = \frac{G_s}{\rho} \tag{2.19}$$

3. Calculate the shell side equivalent diameter

For an equilateral triangular pitch arrangement:

$$d_e = \frac{1.27}{d_o}(p_t^2 - 0.917 d_o^2) \tag{2.20}$$

4. Calculate the shell side Reynolds number

$$Re = \frac{\rho d_e u_s}{\mu} \tag{2.21}$$

5. For the calculated Reynold number, read the value of j_h from Figure 2.30 for the selected baffle cut and tube arrangement, and the calculate the shell-side heat transfer coefficient h_s from

$$Nu = \frac{h_s d_e}{k_f} = j_h Re Pr^{1/3} \left(\frac{\mu}{\mu_w}\right)^{0.14} \tag{2.22}$$

The tube wall temperature can be estimated using the method given for the tube-side.

6. For the calculated shell side Reynold number, read the friction factor from Figure 2.31 and calculate the shell side pressure drop from:

$$\Delta P_s = \left(8 \times j_f \times \frac{D_s}{d_e} \times \frac{L}{l_B} \times \frac{\rho u_s^2}{2}\right) \tag{2.23}$$

2.3.1.11 Condenser

The construction of a condenser will be similar to other shell and tube exchangers, but with a wider baffle spacing, typically $l_B = D_s$. Condenser is similar to shell and tube heat exchanger but it is difference in heat transfer coefficients. Dropwise

condensation will give higher heat transfer coefficients. Condenser is separated in 4 types.

Four condenser configurations are possible:

1. Horizontal, with condensation in the shell, and the cooling medium in the tubes.
2. Horizontal, with condensation in the tubes.
3. Vertical, with condensation in the shell.
4. Vertical, with condensation in the tubes.

2.3.1.11.1 Condensation Outside Horizontal Tubes

As discuss above, the heat transfer coefficient which condense outside horizontal tubes is calculated in difference way from shell and tube heat exchanger because condensate is un-predicable. So, the heat transfer coefficient is calculated by using Kern's method.

$$h_o = 0.95 \times k_L \times \left(\frac{\rho_L \times (\rho_L - \rho_v) \times g}{\mu_L \times \Gamma_h}\right)^{-1/3} \times N_r^{-1/6} \quad (2.24)$$

2.3.2 Scrubber [Christie John Geankoplis, R.K. Sinnott]

Absorption or scrubber is the separation process which is used when the two contacting phases are a gas and a liquid. A solute is absorbed from the gas phase by using liquid in absorption. In this project, benzoic acid is absorbed by 6.7 wt% sodium hydroxide solution.

2.3.2.1 Gas-Liquid Equilibrium

Gas-liquid equilibrium data is found by experimental, literature and Henry's law. However, Henry's law is normally used because it is easy method. Henry's law is equilibrium relation between p_A in the gas phase and x_A can be expressed by a straight-line Henry's law equation at low concentrations (less than 0.010 wt%):

$$p_A = Hx_A \quad (2.25)$$

2.3.2.2 Operating-Line Derivation

When the liquid absorbs solute A at the higher stage, the liquid at middle stage is high concentration. Then it passes thorough the lower stage to absorb solute A again. So, the operating line shows that how liquid absorb in that stage and leach to equilibrium. The operating-line equation for a paced tower is:

$$L'\left(\frac{x_2}{1-x_2}\right) + V'\left(\frac{y_1}{1-y_1}\right) = L'\left(\frac{x_1}{1-x_1}\right) + V'\left(\frac{y_2}{1-y_2}\right) \quad (2.26)$$

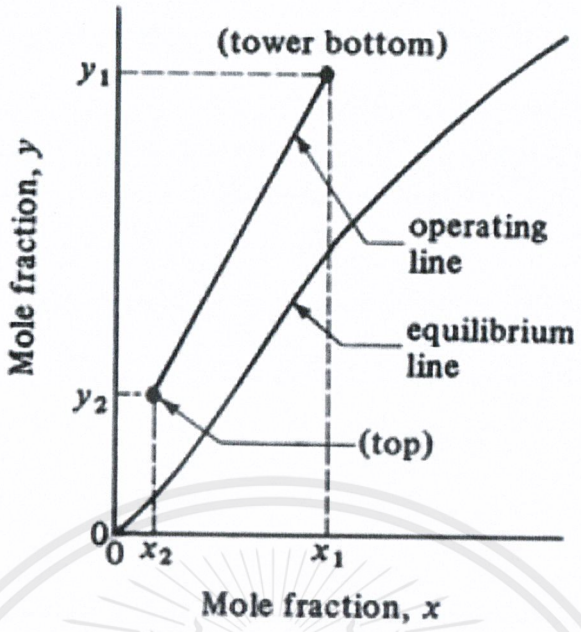

Figure 2.32 Material balance for a countercurrent paced absorption tower [Christie John Geankoplis, 2014]

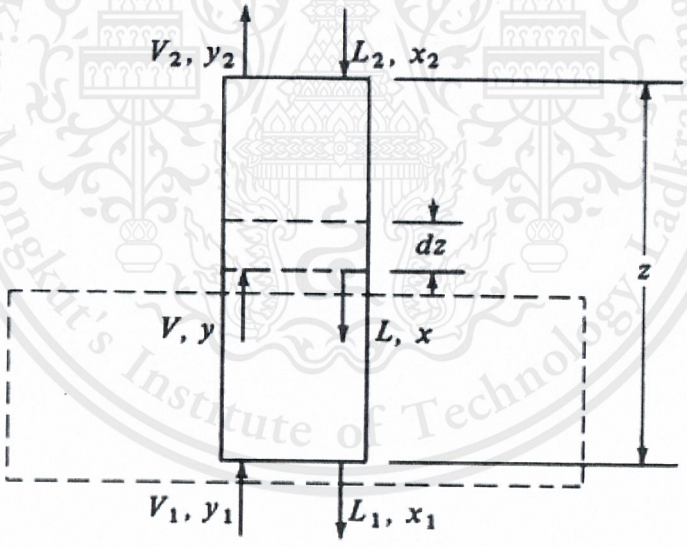

Figure 2.33 Location of operating line for absorption of A from V to L stream [Christie John Geankoplis, 2014]

This equation, when plotted on yx coordinates, will give a curved line, as shown in Figure 2.33.

2.3.2.3 Limiting and Optimum L'/V' Ratios

In the absorption process, the inlet gas flow V_1 (Figure 2.32) and its composition y_1 are generally set. The exit concentration y_2 is also usually set by the designer, and the concentration x_2 of the entering liquid is often fixed by process requirements. Hence, the amount of the entering liquid flow L_2 or L' is open to choose.

In Figure 2.34, the flow V_1 and the concentrations y_2, x_2 and y_1 are set. When the operating line has a minimum slope, and touches the equilibrium line at point P, the liquid flow L' is a minimum at L'_{min}. The value of x_1 is a maximum at x_{1max} when L' is a minimum. At point P the driving forces $y - y^*$, $y - y_i$, $x^* - x$ and $x_i - x$ are all zero. To solve for L'_{min}, the values y_1 and x_{1max} are substituted into the operating-line equation. In some cases, if the equilibrium line is curved concavely downward, the minimum value of L is reached by the operating line becoming tangent to the equilibrium line instead of intersecting it.

The choice of the optimum L'/V' ratio is use in the design depends on an economic balance. In absorption, too high a value requires a large liquid flow and hence a large-diameter tower. A small liquid flow results in a high tower, which is also costly, as an approximation, for absorption the optimum liquid flow rate can be taken as 1.2-1.5 times the limiting rate L'_{min}, with 1.5 usually used.

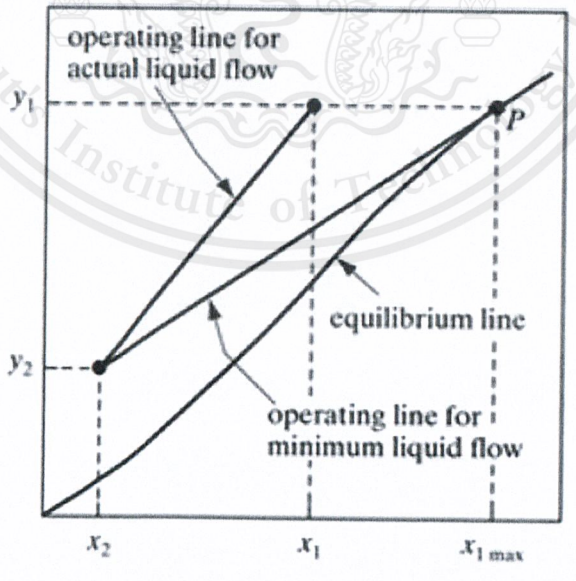

Figure 2.34 Operating line for limiting conditions of absorption

[Christie John Geankoplis, 2014]

2.3.2.4 Absorption in Plate and Packed Towers

Absorption is a mass-transfer process in which a vapor solute A in a gas mixture is absorbed by a liquid in which the solute is more or less soluble. The gas mixture consists mainly of an inert gas and the solute. The liquid also is primarily immiscible in the gas phase; that is, its vaporization into the gas phase is relatively slight.

2.3.2.4.1 Absorption in Plate Tower

Plate is used for increasing efficiency of vapor and liquid into contact. There are several types such as sieve tray which is the very common, valve tray which is higher efficiency than sieve tray, and bubble-cap tray which is the highest efficiency.

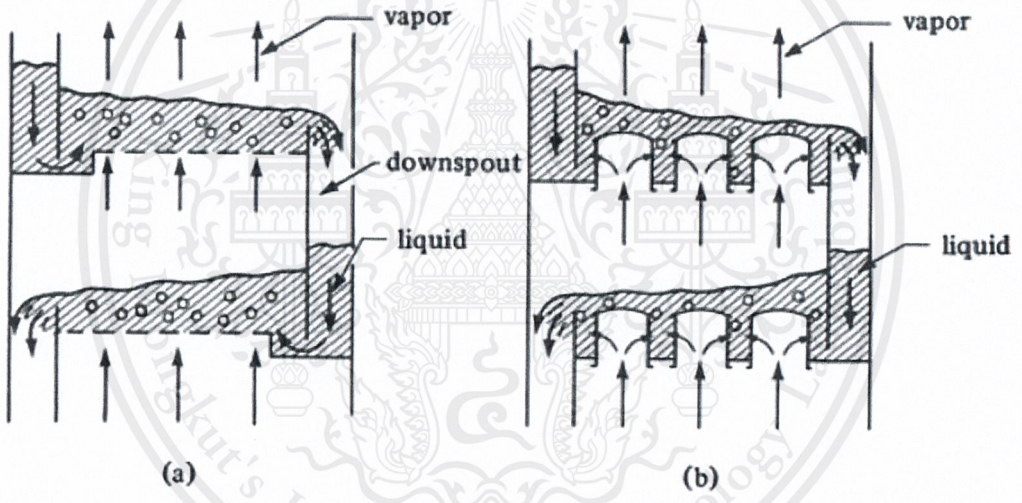

Figure 2.35 Tray contacting devices: (a) detail of sieve-tray tower, (b) detail of valve-tray tower [Christie John Geankoplis, 2014]

2.3.2.4.2 Absorption in Packed Tower

Packed towers are used for continuous countercurrent contacting of gas and liquid in absorption as well as for vapor-liquid contacting in distillation. The tower in Figure 2.36 consists of a cylindrical column containing a gas inlet and distributing space at the bottom, a liquid inlet and distributing device at the top, a gas outlet at the top, a liquid outlet at the bottom and a packing in the tower. The gas enters the distributing space below the packed section and rise upward through the packing mean. On the other hand, liquid flow down to contact with vapor at the packed section.

So, a large area of intimate contact between the liquid and gas is provided by the packing.

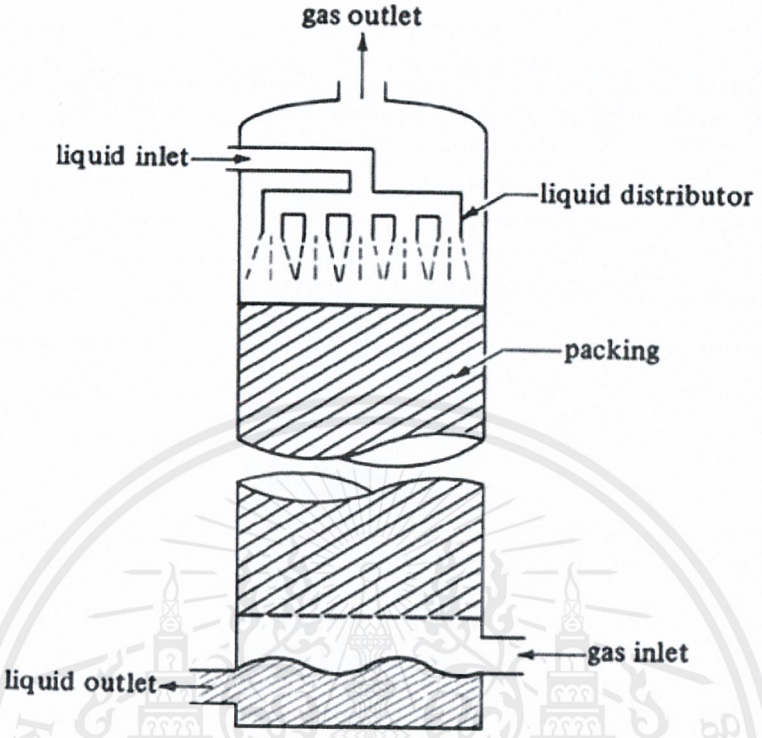

Figure 2.36 Packed tower flows and characteristics for absorption [Christie John Geankoplis, 2014]

Type of Random Packing for Absorption.

Random packing for absorption is developed for a long time and they have several type of random packing. Common types of packing which are dumped at random in the tower are shown in Figure 37.

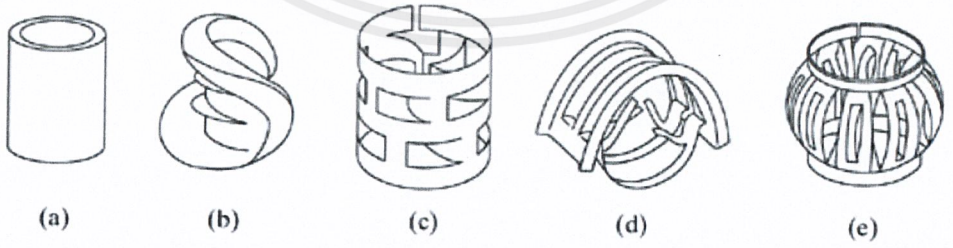

Figure 2.37 Typical random or dumped tower packings: (a) Raschig ring; (b) Berl saddle; (c) Pall ring; (d) Intalox metal, IMTP; (e) Jaeger Metal Tri-Pack. [Christie John Geankoplis, 2014]

The efficiency of random packed is higher from old type (a) to new type (e), respectively. Most of the tower packings are made of materials such as clay, porcelain, metal, or plastic. High void spaces of 65-95% are characteristic of good packings. The packings permit relatively large volumes of liquid to pass countercurrent to the gas flow through the openings with relatively low pressure drops for the gas.

2.3.2.4.3 Pressure Drop and Flooding in Packed Towers

In a given packed tower with a given type and size of packing and with a definite flow of liquid, there is an upper limit to the rate of gas flow, called the flooding velocity. Above this gas velocity the tower cannot operate. At low gas velocities, the liquid flows downward through the packing, essentially uninfluenced by the upward gas flow. As the gas flow rate is increased at low gas velocities, the pressure drop is proportional to the flow rate to the 1.8 power. At a gas flow rate called the loading point, the gas starts to hinder the liquid downflow, and local accumulations or pools of liquid start to appear in the packing. The pressure drop of the gas starts to rise at a faster rate. As the gas flow rate is increased, the liquid holdup or accumulation increases. At the flooding point, the liquid can no longer flow down through the packing and is blown out with the gas.

In an actual, operating tower, the gas velocity is well below flooding. The optimum economic gas velocity is about one-half or more of the flooding velocity. It depends upon a balance of economic factors including equipment cost, pressure drop, and processing variables. Pressure drop in the packing is an important consideration in design of a tower and is covered in detail below.

Pressure Drop in Random Packings

The empirical correlations of random packings are based on experimental data. It is used to predict the pressure drop in the gas flow. The empirical correlations have been plotted by Strigle which shown in Figure 2.38. The line for ΔP = 2.0 in. H_2O/ft has been extrapolated. The ordinate (capacity parameter) is $v_G[\rho_G/(\rho_L - \rho_G)]^{0.5} F_p^{0.5} v^{0.05}$ and the abscissa (flow parameter) is $\left(\frac{G_L}{G_G}\right)\left(\frac{\rho_G}{\rho_L}\right)^{0.5}$. Note that this capacity parameter is not dimensionless and that only these units should be used. This correlation predicts pressure drops to an accuracy of 11% deviation. The packing factor F_p is almost inversely proportional to packing size. This packing factor

is determined empirically for each size and type of packing, and some data are given in Table 2.6.

Flooding Pressure Drop in Packed and Structured Packings

It is important for proper design to be able to predict the flooding pressure drop in towers and, hence, the limiting flow rates at flooding. Kister and Gill have developed and empirical equation to predict the limiting pressure drop at flooding. This equation is

$$\Delta P_{flood} = 0.115 F_p^{0.7} \tag{2.27}$$

This can be used for packing factor from 9 up to 60. At a packing factor of 60 or higher, the pressure drop at flooding can be taken as 2.00 in. H_2O/ft.

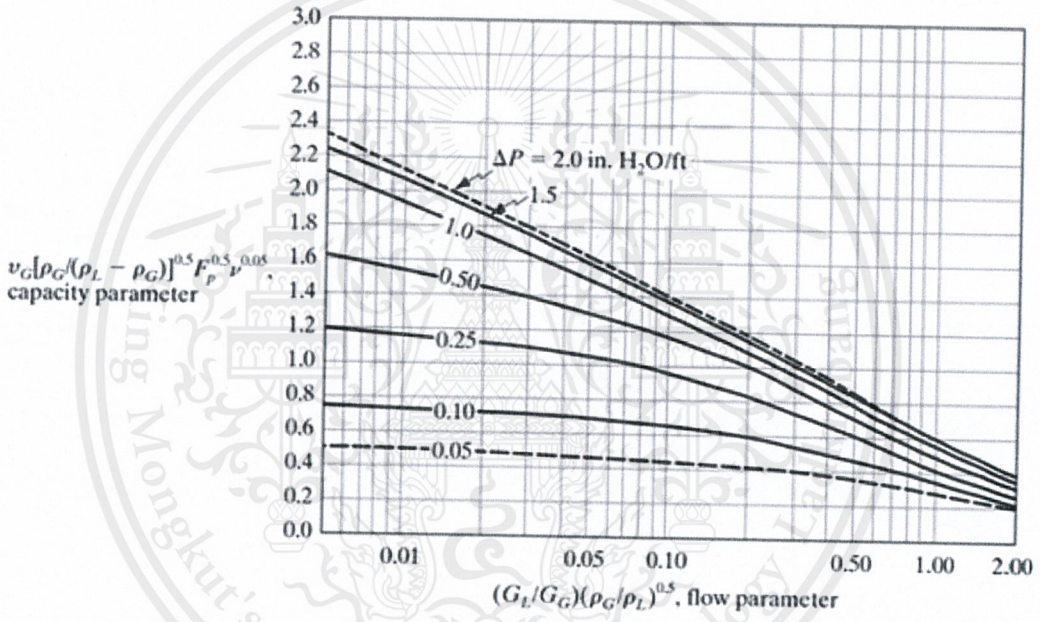

Figure 2.38 Pressure-drop correlation for random packings by Strigle [Christie John Geankoplis, 2014]

The following procedure can be used to determine the limiting flow rates and the tower diameter.

1. First a suitable random packing or structured packing is selected, given an F_p value.
2. A suitable liquid-to-gas ratio is selected along with the total gas flow rate.
3. The pressure drop at flooding is calculated using flooding equation, or if F_p is 60 or over, the ΔP_{flood} is taken as 2.0 in./ft packing height.
4. Then the flow parameter is calculated, and using the pressure drop at flooding and either Figure 2.38, the capacity parameter is read off the plot.

5. Using the capacity parameter, the value of G_G is obtained, which is the maximum value at flooding.
6. Using a suitable % of the flooding value of G_G for design, a new G_G and G_L are obtained. The pressure drop can also be obtained from Figure 2.38.
7. Knowing the total gas flow rate and G_G, the tower cross-sectional area and ID can be calculated.

Table 2.6 Design data for various packings [Christie John Geankoplis, 2014]

	Size		Bulk Density (kg/m^3)	Surface (m^2/m^3)	Packing Factor F_p m^{-1}
	in	mm			
Raschig rings ceramic	0.50	13	881	368	2100
	1.0	25	673	190	525
	1.5	38	689	128	310
	2.0	51	651	95	210
	3.0	76	561	69	120
Metal (density for carbon steel)	0.5	13	1201	417	980
	1.0	25	625	207	375
	1.5	38	785	141	270
	2.0	51	593	102	190
	3.0	76	400	72	105
Pall rings metal (density for carbon steel)	0.625	16	593	341	230
	1.0	25	481	210	160
	1.25	32	385	128	92
	2.0	51	353	102	66
	3.5	76	273	66	52
Plastics (density for polypropylene)	0.625	16	112	341	320
	1.0	25	88	207	170
	1.5	38	76	128	130
	2.0	51	68	102	82
	3.5	89	64	85	52
INTALOX® saddles ceramic	0.5	13	737	480	660
	1.0	25	673	253	300
	1.5	38	625	194	170
	2.0	51	609	108	130
	3.0	76	577		72

For design of absorption, the ratio of tower diameter to packing size should be 10/1 or greater. This is to ensure good liquid and gas distribution. Random-packed towers are generally used only for diameters of 1.0 m or less. Tray tower less than 0.6 m in diameter are usually not used because of cleaning and access problems. So, in this project random-packed tower are chosen. Finally, absorption tower should be designed using about 50 – 70% of the flooding velocity, with the high value used at high flow parameters.

2.3.2.5 Column Height [R.K. Sinnott, 2005]

For design purposes, term of "transfer units" (HTU) is written in short form.

$$Z = H_{OG}N_{OG} \tag{2.28}$$

$$H_{OG} = H_G + m\frac{G_m}{L_m}H_L \tag{2.29}$$

$$N_{OG} = \frac{1}{1-m\frac{G_m}{L_m}}\ln\left[\left(1 - m\frac{G_m}{L_m}\right)\frac{y_1}{y_2} + m\frac{G_m}{L_m}\right] \tag{2.30}$$

So, the column height is calculated by using Cornell's method which is shown below.

2.3.2.5.1 Cornell's method

Cornell *et al.* reviewed the previously published data and presented empirical equations for predicting the height of the gas and liquid film transfer units. Their correlation takes into account the physical properties of the system, the gas and liquid flow rates, and the column diameter and height. Equations and figures are given for a range of sizes of Rasching rings and Berl saddles. Only those for Berl saddles are given here, as it is unlikely that Raschig rings would be considered for a new column. Though the mass-transfer efficiency of Pall rings will be higher than that of the equivalent size Berl saddle, the method can be used to make conservative estimates for these packings.

Cornell's equations are

$$H_G = 0.011\Psi_h {Sc_v}^{0.5}\left(\frac{D_c}{0.305}\right)^{1.11}\left(\frac{Z}{3.05}\right)^{0.33}/(L_W^* f_1 f_2 f_3)^{0.5} \tag{2.31}$$

$$H_L = 0.305\phi_h {Sc_L}^{0.5} K_3\left(\frac{Z}{3.05}\right)^{0.15} \tag{2.32}$$

Suffix w refers to the physical properties of water at 20 ^{O}C

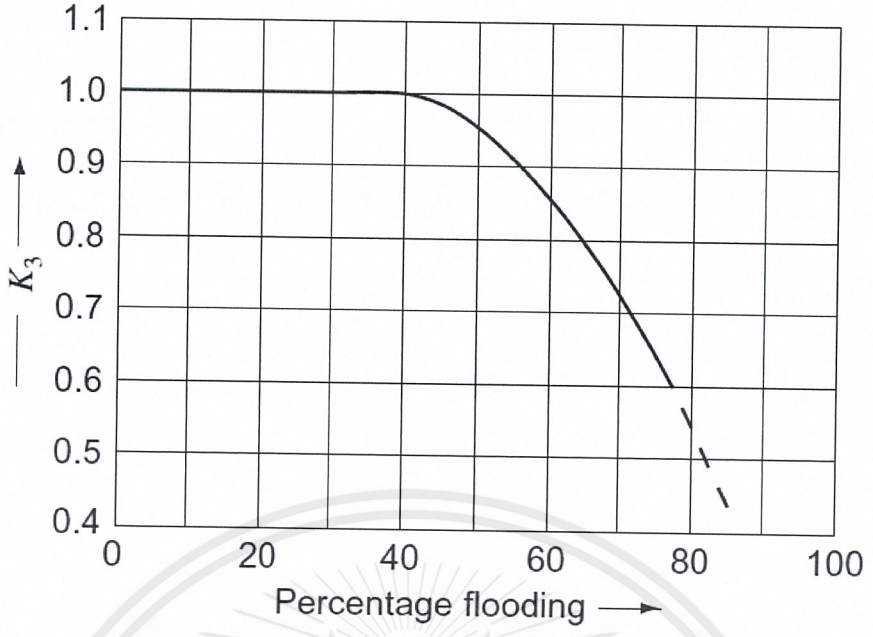

Figure 2.39 Percentage flooding correction factor [R.K. Sinnott, 2005]

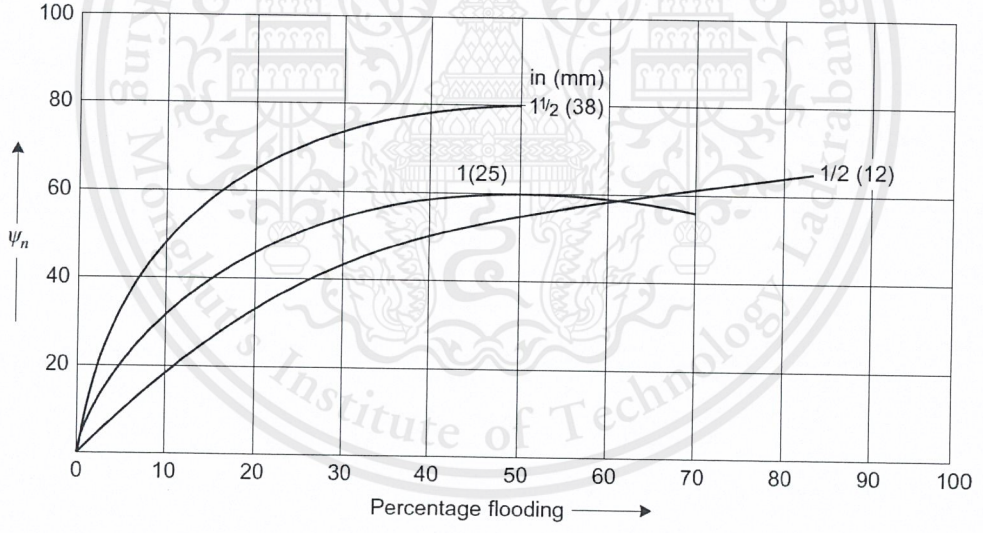

Figure 2.40 Factor H_G for Berl saddles [R.K. Sinnott, 2005]

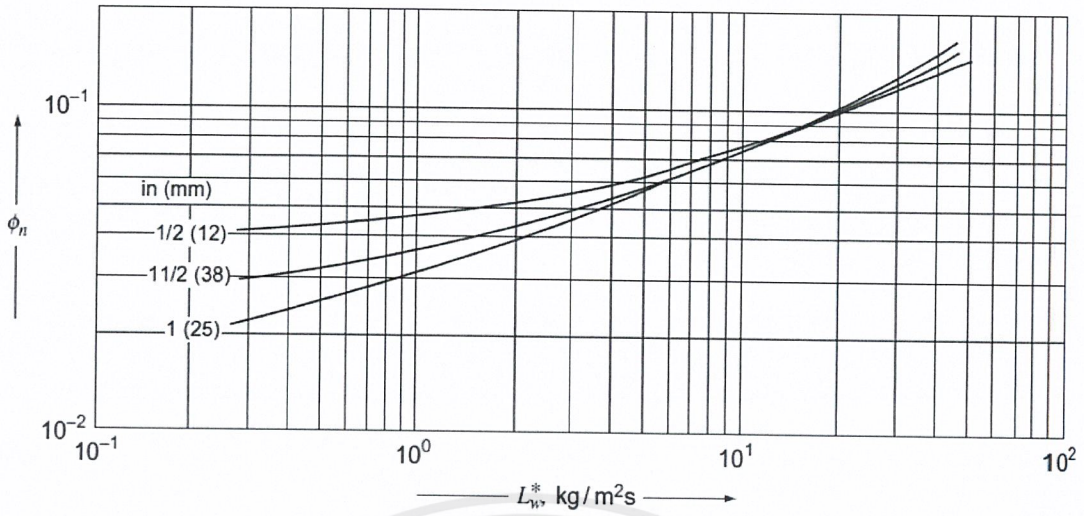

Figure 2.41 Factor for H_L for Berl saddles [R.K. Sinnott, 2005]

The term (D_C/0.305) and (Z/3.05) are included in the equation to allow for the effects of column diameter and packed-bed height. The "standard" values used by Cornell were 0.305 m for diameter, and 3.05 m for height. These correction terms will clearly give silly results if applied over too wide a rage of values. For design purposes the diameter correction term should be taken as a fixed value of 2.3 for columns above 0.6 m diameter, and the height correction should only be included when the distance between liquid redistributors is greater than 3 m. To use Figure 2.39 and 2.40 an estimate of the column percentage flooding is needed which calculated from flooding section.

CHAPTER III
RESEARCH METHODOLOGY

3.1 Hydrogen & Impurities Balances

3.1.1 Hydrogen Consumption in Reactor

To calculate hydrogen consumption in reactor, many methods are offered such as kinetic method, simulation method, and stoichiometry method. However, Stoichiometry method is the easiest way to calculate the hydrogen consumption.

Stoichiometry Calculation

$$4 - CBA + 2H_2 \rightarrow p - TA + H_2O$$

The calculation is shown in appendix A. As Figure 3.1, hydrogen is consumed in the reactor to convert 4-CBA from 3000 ppm to less than 15 ppm. For the calculation, it should calculate at 100% conversion because it is the worth case which excess hydrogen is the least of calculation. This calculation is based on average data from 11/02/2016 to 14/08/2016 which is the normal operation time. Then, it is assumed that all of excess hydrogen will release at crystallizer and preheater, respectively.

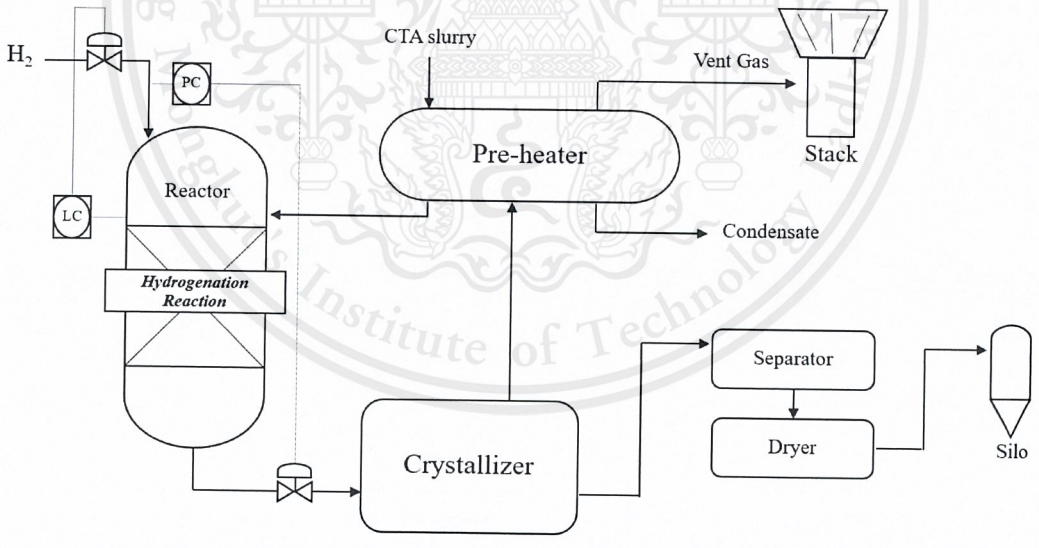

Figure 3.1 Hydrogenation process for PTA production

3.1.2 Sampling the impurities

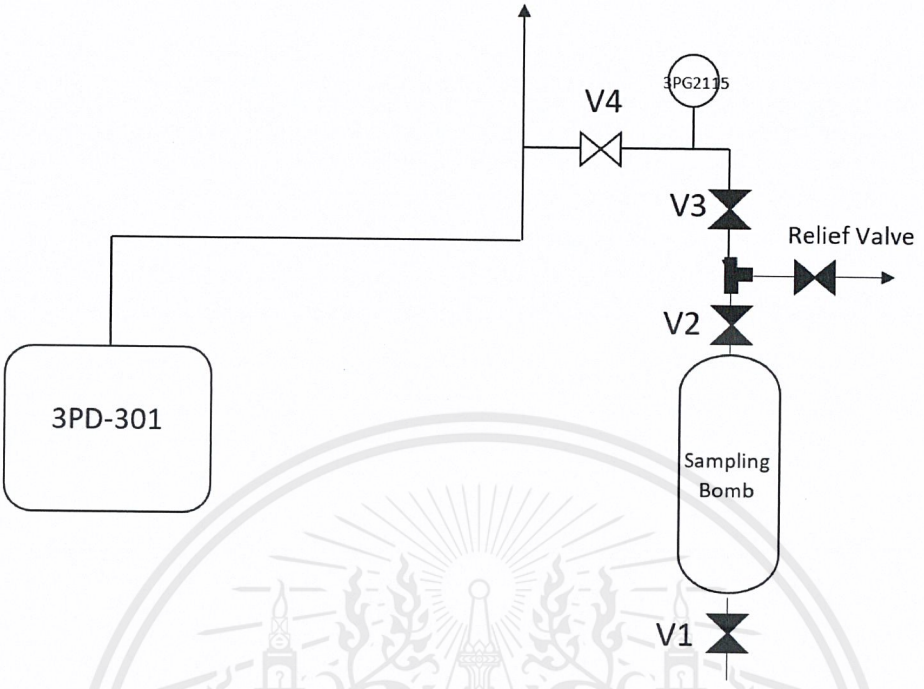

Figure 3.2 Sampling device which is connected to the process

As shown in Figure 3.2, the sampling device is connected with the pressure gauge. The sampling device is desired for keep the sampling in gas phase. It withstands for high temperature and high pressure. Then, the objective is to keep the sampling for measure the % impurities which the procedure is described below.

Procedure

1. Check every device to confirm it is ready to use.
2. Reduce pressure by closing valve V4 (Read the pressure gauge that it is 0 barg).
3. Close valve V3 and connect the sampling device.
4. Open valve V1, V2 and V3 while still open valve v4.
5. Open valve slowly V4 and read the pressure gauge to be 1 barg.
6. Purging for 5 minute.
7. Close valve V1 slowly. Then it makes the pressure.
8. Read off the pressure at pressure gauge from 1 barg to 2 barg.
9. Close valve V3 and reduce pressure by open release pressure valve.
10. Disconnect sampling device from the process.
11. Open Valve V4 and close valve V3 for turn it to normal operation.

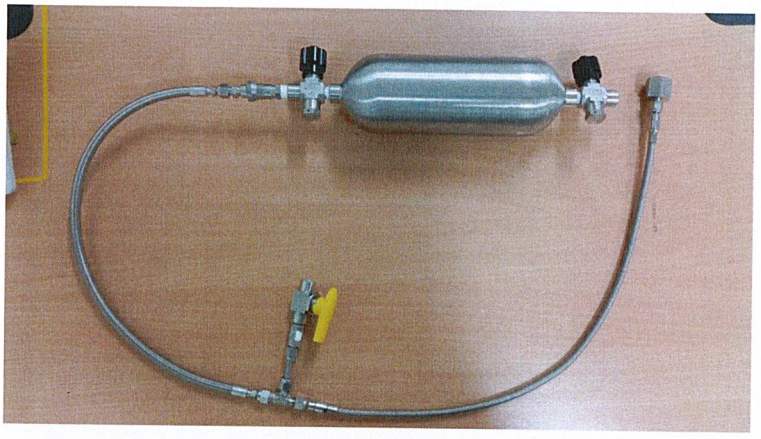

Figure 3.3 Sampling device for high pressure gas stream

3.2 Choosing Technology [David Parker, Tan Wei industry, YAN Yi-wei]

For recovery hydrogen, many technology are considered. They are compared advantages and disadvantages. However, the technology which is chosen must be the lowest investment (CAPEX and OPEX). So, the pressure swing adsorption, membrane separation and cryogenic separation are considered.

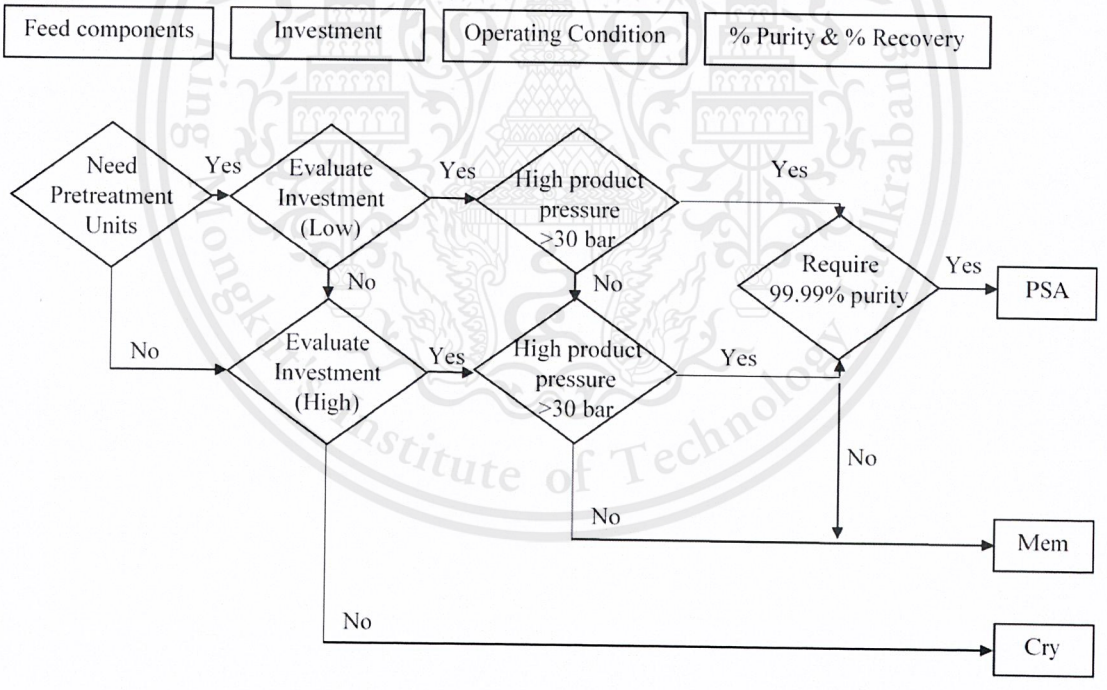

Figure 3.4 Choosing technology chart

Not only choosing technology chart, but also Table which compared advantages and disadvantages of hydrogen recovery technology is used together to choosing technology.

3.3 Design Process Overview

When the pressure swing adsorption is chosen because low investment and high % purity, the pretreatment unit is required. Many impurities such as terephthalic acid powder affect to pressure swing adsorption operation. It may be shorter operation time. Then condenser is required for remove water, terephthalic acid, *p*-toluic acid and 4-carboxy benzaldehyde. Scrubber is required to remove benzoic acid. Finally, pressure swing adsorption is used for remove CO, CO_2 and N_2. This design is based on patent which is used in PTA production plants.

3.3.1 Condenser Design

Condenser is designed following design procedure as shown in Figure 3.5. The example of calculation is shown in appendix B.

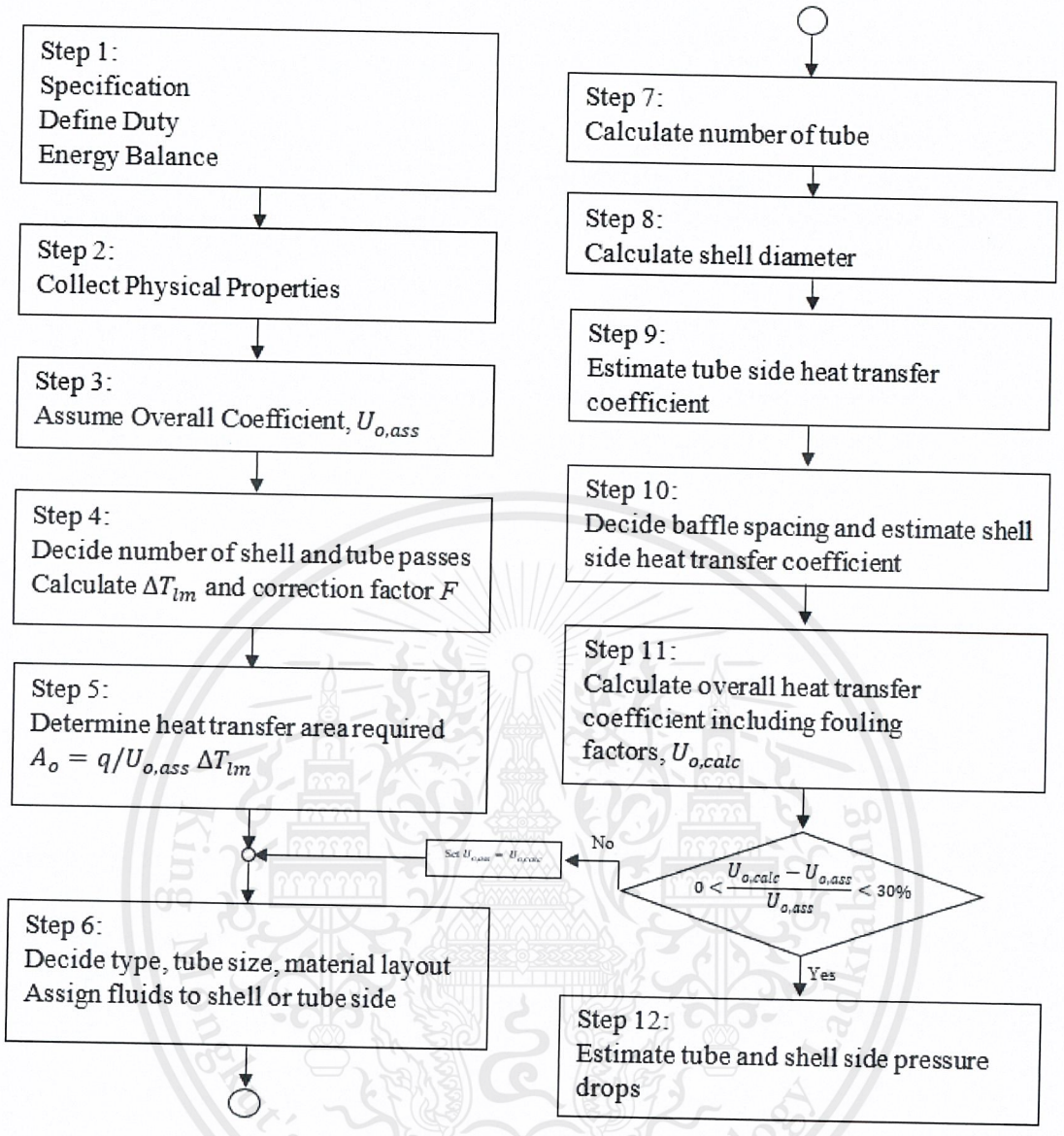

Figure 3.5 Design procedure for shell and tube heat exchanger and condenser

3.3.2 Scrubber Design

Scrubber is designed following design procedure as shown in Figure 3.6. The example of calculation is shown in appendix C.

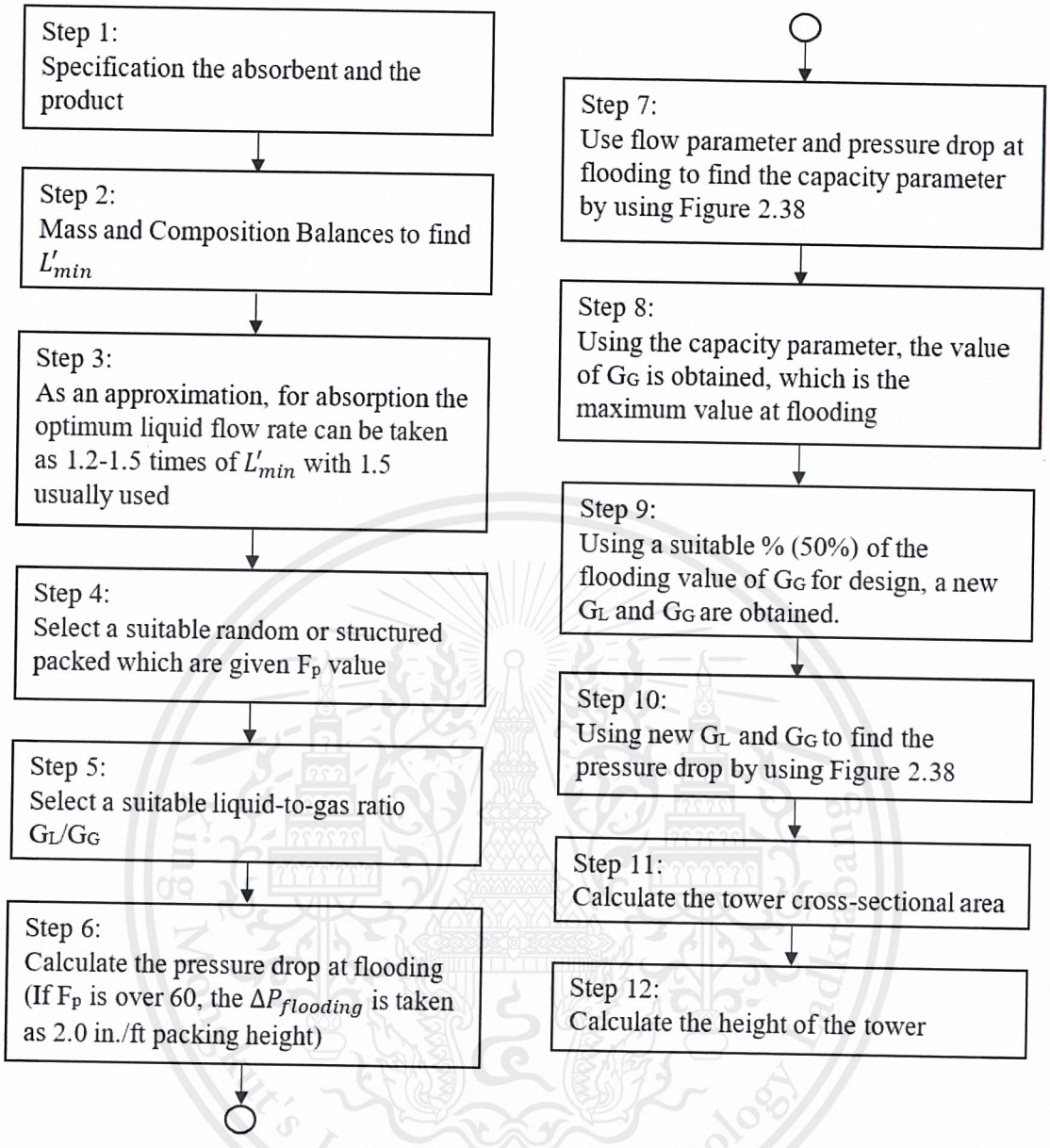

Figure 3.6 Design procedure for scrubber

3.3.3 Pressure Swing Adsorption Design

Pressure swing adsorption is designed based on assumption of *Dong-Kyu Moon Applied Energy 183(2016), 760-774.* The example of design is shown in appendix D. However, the literature is design by using 2 bed for recovery hydrogen but it is not enough for industrial scale. For industrial scale, it requires at least 4 bed for continuous process and more than 4 bed for spare in some emergency case. Then this project requires the lowest investment. So 4 bed is designed in this study.

CHAPTER IV
RESULTS AND DISCUSSION

The technology is chosen from Choosing technology chart (Figure 3.4) and comparing technology chart (Table 4.1), that pressure swing adsorption is the best technology to recover hydrogen for PTA production plant. All of technology require pretreatment unit. However, only pressure swing adsorption is the lowest investment, keep high product pressure and qualities on specification.

Table 4.1 Comparing technology chart

Features	PSA	Polymeric-Membrane	Pd-Membrane
Qualities	99.99% purity 90% recovery (Guarantee 85% recovery)	98% purity 95% recovery	99.99% purity 95% recovery
Operating Conditions	10-40 bar	>20 bar	>20 bar
Product Pressure (Target >30 bar)	Near the feed pressure	Need a compressor ($\Delta P = 20$ bar)	Need a compressor ($\Delta P = 20$ bar)
References	More than 4 patents (1 PTA plant use)	Some industries	No large scale reference (Laboratory scale)
Investment* (Estimated)	14 MBaht	15 MBaht	>15 MBaht

Note* It is estimated from journal, Ali Muvechain,2013]

When pressure swing adsorption is chosen, the design process to recovery hydrogen is based on patent. It requires pretreatment units which are condenser and scrubber. The condenser is designed as shown in Figure 4.1. Then scrubber is designed as shown in Figure 4.2. Finally, pressure swing adsorption is designed as shown in Figure 4.3.

4.1 Condenser design

The condenser is designed to remove water, terephthalic acid, *p*-toluic acid and 4-carboxy benzaldehyde. To remove water, it is removed by condense water in gas phase to liquid phase. As water condense, terephthalic acid, *p*-toluic acid and 4-carboxy benzaldehyde also removed together with water in liquid phase. It requires duty to condense steam is around 13,000,000.00 kJ/h. The area of condenser is 116.76 m^2. The type of condenser is split ring floating head because it is withstand for high pressure. For more information is shown in Figure 4.1.

	Condenser Data Sheet							
1	Type		Split Ring Floating Head					
2	Shell		1		Tube	4		Pass
	Performances							
3	Descriptions		Shell Side			Tube Side		
4	Fluid Circulated		Steam+Hydrogen+Impurities			CCW		
5	Temperature	Inlet	250.00		°C	32.00		°C
6		Outlet	54.00		°C	80.00		°C
7	Operating Pressure		40.00		bar	1.00		bar
8	Total Fluid Entering		5,190.00		kg/h	66,549.58		kg/h
9	Fouling Resisteance		Steam	0.00	$(W/m^2\,^oC)^{-1}$	CCW	0.00	$(W/m^2\,^oC)^{-1}$
10	Velocity		4.59		m/s	1.10		m/s
11	Pressure Drop		0.03		bar	0.29		bar
12	Heat Exchange		13,362,090.96					kJ/h
13	Overall Heat Transfer Coefficient		552.61					$W/m^2\,^oC$
	Constructions							
14	Tube	Inside Diameter	0.01	m				
15		Outside Diameter	0.02	m				
16		Number of Tube	390.04					
17		Pitch Type	Triangular Pitch					
18		Pitch	0.02	m				
19	Shell	Inside Diameter	0.62	m				
20		%Cut	45.00	%				
21		Baffle Spacing	0.62	m				
22	Number of Tube in Centerrow		23.40					
23	Heat Transfer Area		116.76	m^2				

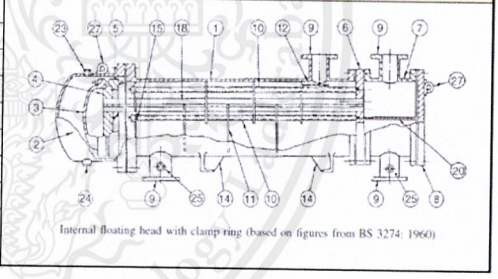

Figure 4.1 Condenser data sheet

4.2 Scrubber design

Scrubber is required to remove benzoic acid. Anyway, scrubber also remove other impurities which drain out with gas from condenser. So, it is used for remove any impurities in solid phase and liquid phase which affect to pressure swing adsorption operation. The scrubber use NaOH as solvent for effectively remove. The high of scrubber is 0.5 m and diameter is 0.42 m. For more information is shown in Figure 4.2.

Scrubber Data Sheet					
Design Absorption	90.00	%			
Vapor Flow Rate	11.01	kg/h	BA in	1.51	kg/h
Liquid Flow Rate	7.44	kg/h	BA out	0.15	kg/h
NaOH	0.50	kg/h			
Design Scrubber					
Type of Packing	Berl Saddles				
Material	Ceramic				
Pressure Drop	0.00053	bar			
Inlet Water Temp.	32.00	°C			
Outlet Water Temp.	50.39	°C			
Diameter	0.42	m			
Height	0.50	m			
Size	0.01	m			
Packed Crossectional Area	0.14	m^2			

Figure 4.2 Scrubber data sheet

4.3 Pressure swing adsorption design

Pressure swing adsorption is used for remove CO, CO_2 and N_2. The product from pressure swing adsorption is 99.99% hydrogen purity and 85% recovery. It uses activated carbon 130 kg and 35 kg for a vessel. The diameter and height of pressure swing adsorption are 0.25 and 1.8 m, respectively. However, pressure swing adsorption requires 4 vessels for continuous process. For more information is shown in Figure 4.3.

PSA Data Sheet				
Breakthrough Curves for AC:LiX=8:2 at 35 bar and 5 LSTP/min				
Time (S)	C/Co	Packed Bed Diameter	2.10	cm
0.00	0.00	Length	100.00	cm
100.00	0.00	Feed	5.00	NL/M
200.00	0.00	**Compositions**		
300.00	0.00	Hydrogen	89.00	mol%
400.00	0.00	Carbon monoxide	3.00	mol%
475.00	0.10	Nitrogen	6.00	mol%
500.00	0.80	Carbon dioxide	2.00	mol%
525.00	1.00	Molecular Weight	5.18	g/mol
600.00	1.00	Temperature	35.00	°C
700.00	1.00	Pressure	35.00	bar
800.00	1.00	Density	1.37	kg/m^3
900.00	1.00	Break point time (0.01)	475.00	s
Design				
Zeolite	35.15			kg
Activated Carbon	130.07			kg
Diameter	0.25			m
Height	1.80			m
Packed Bed Volume	0.09			m^3
Pressure	35.00			bar
Temperature	50.39			°C

Adsorben Properties			
Feature	Unit	Zeolite Lix	Activated Carbon
Type	-	Pellet	Cylindircal
Particle Size d_p	mm	1.5-1.7	1.7-2.4
Particle Density	g/cm^3	1.05	0.75
Skeletal Density	g/cm^3	2.00	1.85
Apparent Density	g/cm^3	0.72	0.54
Bed Porosity	-	0.31	0.28
Total Porosity	-	0.64	0.71
Heat Capacity	J/kg K	1,070.00	1,570.00
Pore Volume	cm^3/g	0.39	0.46
Total Surface Area	m^2/g	664.70	1,306.40

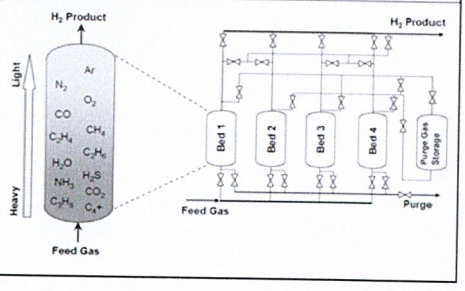

Figure 4.3 PSA data sheet

The data sheet as shown in Figure above is preliminary design for estimate cost by sending detail to vendor. The estimate cost is next step of this project.

CHAPTER V
CONCLUSION

5.1 Conclusion

Feasibility study of hydrogen recovery from PTA production process was studied. The excess hydrogen lost at the stack was found to be 5.3 MBath/year. Hydrogen recovery unit (HRU) consisting of condenser, scrubber and 4 vessels of pressure swing adsorption was designed. The condenser and scrubber are used for pre-treatment of the impurities from PTA production. The condenser separates water, terephthalic acid, *p*-toluic acid and 4-carboxy benzaldehyde while the scrubber separates BA. Four vessels of pressure swing adsorption are used for hydrogen recovery and for the removal of CO, CO_2 and N_2. The detail design is shown in Table 5.1. Hydrogen (99.99 %purity, 5.7 kg/h) of approximately 85 wt% was recovered. The estimated saving cost is 3.8 MBaht/year.

Table 5.1 Design conclusion

Design	Condenser	Scrubber	PSA
Temperatures	Inlet = 250 °C Outlet = 60 °C	Inlet = 60 °C Outlet = 55 °C	Inlet 50 °C Outlet 50 °C
Pressure Drop (Feed = 40 bar)	ΔP = 0.18 bar	ΔP = 0.00052 bar	–
Length/Height	5 m	0.5 m	1 m
Diameter	Shell Inside Diameter = 0.6 m	0.3 m	0.25 m
Chemicals make-up	CCW	NaOH & CCW	Activated Carbon & Zeolite LiX
Materials	Stainless Steel 304	Berl Saddle	-

REFERENCES

1. Abbas Azarpour, Gholamreza Zahedi. Performance Analysis of Crude Terephthalic Acid Hydropurification in an Industrial Trickle-bed Reactor Experiencing Catalyst Deactivation. *Chemical Engineering Journal*. 2012, 209, pp 180-193.
2. Ali Muvechain and Majid Pakizeh. Hydrogen Recovery from Tehram Refinery Off-Gas Using Pressure Swing Adsorption, Gas Absorption and Membrane Separation Technologies: Simulation and Economic Evaluation. *Korean J. Cehm Eng.*, 2013, 30, 937-948.
3. Christie John Geankoplis. *Transport Processes & Separation Process Principles (Includes Unit Operations)*, 4nd ed.; Pearson: England, pp 625-777
4. Coulson and Richardson's. Chemical Engineering., 5th ed.; Butterworth Heinemann, 2002; Vol 2, pp 970-1049.
5. David Parker, Fiona Mary Campbell, Andrew Harrison. Process for Recovering Hydrogen in Producing Pure Terephthalic Acid. US patent no. 6407286B1, June 2002
6. Dong-Kyu Moon, Dong-Geun Lee, Chang-Ha Lee. H_2 Pressure Swing Adsorption for High Pressure Syngas from an Integrated Gasification Combined Cycle with a Carbon Capture Process. *Applied Energy*. 2016, 183, pp 760-774.
7. Gazzani Matteo. Hydrogen Production: Membranes and Conventional Technologies. Separation Processes Laboratory. 20.11.2015.
8. Itsuki Uehara. Separation and Purification of Hydrogen. *Energy Carriers and Conversion Systems*. Vol 1. National Institute of Advanced Industrial Science and Technology. Japan.
9. Johnson Matthey Process Technologies, Purified Terephthalic Acid (PTA). http://davyprotech.com. (Access August, 2016)
10. Logan Scott McLeod. Hydrogen Permeation Through Microfabricated Palladium-Silver Alloy Membranes. School of Mechanical Engineering Georgia Institute of Technology. 2008.
11. Nitin Patel, Bill Baade. Creating Value Through Refinery Hydrogen Management. Singapore. 2006.

12. R.K. Sinnott. *Chemical Engineering Design*, 4th ed.; Elsevier: Oxford, 2005; Vol. 6, pp 493-790.

13. S. Tourani, A.A. Safekordi, M. Rashidzadeh, A.M. Rashidi, F. Khorasheh. Hydrogenation of Crude Terephthalic Acid by Supported Pd and Pd-Sn Catalysts on Functionalized Multiwall Carbon Nanotubes. *Chemical Engineering Research and Design*. 2016, 109, pp 41-52

14. Tan Wei industry. Method for Recycling Hydrogen from Refined Benzene Dicarboxylic Acid Plant Discharge Air Flow. CN patent no. 101475462B, Jan 2012.

15. The Linde Group. Hydrogen Recovery by Pressure Swing Adsorption. http:// linde-engineering.uy. (Access August, 2016)

16. YAN Yi-wei, WANG Jian-ping, YAN Guo-wei. Hydrogen Recycling Device in PTA (Purified Terephthalic Acid) Production Technology. CN patent no. 204039055U, Dec 2014.

17. Zajra Rabiei. Hydrogen Management in Refineries. *Petroleum & Coal*. 2012, 54, 357-368.

18. Zhi Li, Weimin Zhong. Xiaoquiang Wang, Na Luo, Feng Qian. Control Structure Design of and Industrial Crude Terephthalic Acid Hydropurification Process with Catalyst Deactivation. *Computer and Chemical Engineering*. 2016, 88, pp 1-12.

APPENDIX

Appendix A

Hydrogen Balance

Appendix A shows the calculation of hydrogen consumption in reactor and steam flash calculation at crystallizer.

Hydrogen Consumption in Reactor

- Stoichiometry Calculation

$$4-CBA+2H_2 \rightarrow p-TA+H_2O$$

$$0.32\% \times TA\ feed \times \frac{1mol}{150g} \times \frac{1000\ g}{1\ kg} \times \frac{1000kg}{1\ T}$$

$$= \frac{x\ m^3 \cdot mol}{22.4\ L} \times \frac{1000\ L}{1\ m^3} \times \frac{1\ 4-CBA}{2\ H_2}$$

Where this equation based on 100% conversion of 4-CBA. 4-CBA is calculation from specification of 4-CBA in CTA feed which is 0.32% 4-CBA/1 ton CTA feed.

$$0.32\% \times 80.75 \times \frac{150 \times mol}{g} \times \frac{1000\ g}{1\ kg} \times \frac{1000kg}{1\ T}$$

$$= \frac{x\ m^3 \cdot mol}{22.4\ L} \times \frac{1000\ L}{1\ m^3} \times \frac{1\ 4-CBA}{2\ H_2}$$

$$x = 77.17\ m^3/h$$

Then, hydrogen consume 77.17 m^3/h in reactor.

Vent hydrogen from reactor will flash and dissolve at crystallizer which calculate by flash calculation. However, almost all hydrogen is flashed to heat exchanger but a little of hydrogen is loss by dissolved into the water.

From Figure A, it shows hydrogen solubility of hydrogen in water at different temperature which is calculated at 261 ^{O}C. It is the crystallizer condition.

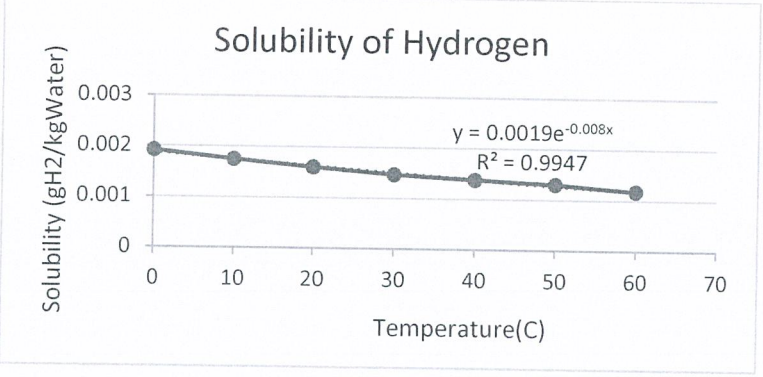

Figure A Solubility of hydrogen in water at different temperature

The solubility of hydrogen at 261 ^{O}C is

$$0.0019e^{-0.008(261)} = 0.000235476\ gH_2/kgH_2O$$

Then, actual water feed 159,152 kg/h. So, hydrogen is loss by solute into the water is

$$0.000235476 \times 159{,}152 = 0.037\ kg/h$$

So, the hydrogen remains 77.17 Nm^3/h which convert to mass is 9.42 kg/h. The hydrogen is flashed 9.42-0.037 = 9.38 kg/h (Hydrogen is flashed 99.6 wt%).

Steam Flash Calculation at Crystallizer

Steam flash calculation is calculated by mass and energy balance. The specific heat formula is

- Specific heat formula

$$Q_i = m_i c_p \Delta T$$

- Heat balance at crystallizer

$$Q_{total} = Q_{in} + Q_{purge} + Q_{crystalline} - Q_{vaporlize} - Q_{out}$$

Overall Energy Balance

Q_{total} is overall energy balance at crystallizer. It is calculated by energy flow in crystallizer plus energy flow in crystallizer by purge water plus energy of crystallization of PTA minus energy vaporization of water minus energy flow out of crystallizer. From the first law of thermodynamic, the overall energy balance must be zero.

Energy Flow in Crystallizer

Q_{in} is energy flow in crystallizer by CTA slurry. The calculation is shown below.

$$Q_{in} = (m_{CTA\ feed} \times c_p \times T_{Reaction\ temperature}) + (m_{actual\ water\ feed} \times H_{water})$$

$$Q_{in} = \left(81{,}644\ kg \times 0.3 \frac{kcal}{°C\ kg} \times 285\ °C\right) + (159{,}152\ kg \times 300\ kcal/kg)$$

$$Q_{in} = 54{,}784{,}793\ kcal$$

Energy Flow in Crystallizer by Purge Water

Q_{purge} is energy flow in crystallizer by purge water. The calculation is shown below.

$$Q_{purge} = (m_{purge\ water\ 1} \times H_{water}) + (m_{purge\ water\ 2} \times H_{water} + (m_{purge\ water\ 3} \times H_{water})$$

$$Q_{purge} = (1000\ kg \times 301.713\ kcal/kg) + (1100\ kg \times 253.554\ kcal/kg) + (200\ kg \times 203.585\ kcal/kg)$$

$$Q_{purge} = 621{,}339\ kcal$$

Energy Crystallization of PTA

$Q_{crystalline}$ is energy crystallization of PTA. The calculation is shown below.

$$Q_{crystalline} = (m_{crystalline\ CTA} \times H_{crystalline\ CTA})$$

$$Q_{crystalline} = ((Actual\ CTA\ feed - Dissolve\ CTA) \times H_{crystalline\ CTA})$$

$$Q_{crystalline} = ((81{,}644 - 23940)\ kg \times 131.6\ kcal/kg)$$

$$Q_{crystalline} = 7{,}592{,}866\ kcal$$

Energy Vaporization of water

$Q_{vaporlize}$ is energy vaporization of water. The calculation is shown below.

$$Q_{vaporlize} = (m_{evap\ water} \times H_{evaporation})$$

$$Q_{vaporlize} = ((Actual\ water\ feed + Purge\ water - Effluent\ water) \times H_{evaporation})$$

$$Q_{vaporlize} = ((159{,}152 + 2{,}301 - Effluent\ water)\ kg \times 668\ kcal/kg)$$

Energy Flow Out of Crystallizer

Q_{out} is energy flow out of crystallizer. The calculation is shown below.

$$Q_{in} = (m_{Actual\ CTA\ Feed} \times c_p \times T_{Reaction\ temperature}) + (Effluent\ water \times H_{water})$$

Then from the energy balance which shown above.

Effluent water = 127,230 kg/h

Steam flash = 31.94 kg/h

Heat Balance in Heat Exchanger

At heat exchanger, hydrogen gas is accumulated. So, the area of tube is reduced. This solution is solved by using line vent gas at heat exchanger. Flash calculation is used for calculate hydrogen and steam loss at this line.

$$Q_{Hot\ side} = Q_{Cold\ side}$$

Energy of hot side

$$Q_{Hot\ side} = Q_{CTA\ solution} + Q_{Water} + Q_{TA}$$

$$Q_{CTA\ solution} = (m_{Dissolve\ CTA} \times H_{CTA\ dissolve})$$

$$Q_{CTA\ solution} = (14{,}868\ kg \times 115.98\ kcal/kg)$$

$$Q_{CTA\ solution} = 1{,}724{,}449\ kcal$$

$$Q_{water} = (m_{Water\ feed} \times \Delta H_{242-203\ ^\circ C})$$

$$Q_{water} = (159{,}152\ kg \times (242 - 203)\ kcal/kg)$$

$$Q_{water} = 6{,}984{,}772\ kcal$$

$$Q_{TA} = (m_{CTA\ feed} \times c_p \times \Delta T_{242-203\ ^\circ C})$$

$$Q_{TA} = \left(81{,}679\ kg \times 0.3 \frac{kcal}{kg\ ^\circ C} \times 39\ ^\circ C\right)$$

$$Q_{TA} = 972{,}308\ kcal$$

$$Q_{Hot\ side} = 1{,}724{,}449 + 6{,}984{,}772 + 972{,}308\ kcal$$

$$Q_{Hot\ side} = 9{,}591{,}528\ kcal$$

Energy of cold side

$$Q_{Hot\ side} = Q_{Latent} + Q_{Sensible\ heat}$$

$$Q_{Hot\ side} = (m_{Water\ feed} \times \Delta H_{Vaporization}) + (m_{steam} \times \Delta H_{Sensible\ heat\ @\ 250^\circ C})$$

$$Q_{Hot\ side} = \left(31{,}940\ kg \times 409.13 \frac{kcal}{kg}\right) + (m_{steam} \times 668.95\ kcal/kg)$$

From the energy balance $Q_{Hot\ side} = Q_{Cold\ side}$, solve for steam flowrate is 5.20 T/h. So, water condense at heat exchanger is 26.75 T/h.

Appendix B

Condenser Design Calculation

Appendix B shows the sample condenser design calculation which is shell and tube exchanger type.

Step 1: Specification

Heat transferred from vapor

Enthalpy of condensation at 250 ^{O}C	=	1715	kJ/kg
Enthalpy of water at 250 ^{O}C	=	1085.7	kJ/kg
Enthalpy of water at 80 ^{O}C	=	335.02	kJ/kg
Enthalpy of water at 54 ^{O}C	=	226.12	kJ/kg
Enthalpy of water at 32 ^{O}C	=	134.1	kJ/kg

$$Q_{Hot} = m\lambda + m(H_{250} - H_{54})$$

$$Q_{Hot} = (5{,}190 \times 1{,}715) + 5{,}190 \times (1{,}085.7 - 226.12) = 1.336 \times 10^{7} kJ$$

From energy balance $Q_{Hot} = Q_{cold}$ and transform the equation.

$$m_{cold} = \frac{Q_{Hot}}{m(H_{80} - H_{32})}$$

$$m_{cold} = 6.6 \times 10^{4}\ kg/h$$

Step 2: Physical Properties

The physical properties of CCW are shown in Table B

Table B Physical properties of CCW

CCW	Inlet	Mean	Outlet	Unit
Temperature	32	56	80	^{O}C
C_P	4.178	4.183	4.197	kJ/kg/^{O}C
k_f	0.615	0.649	0.670	W/m/K
μ	0.798×10^{-3}	0.504×10^{-3}	0.355×10^{-3}	kg/m/s
ρ	996	985.2	971.8	kg/m^3

Step 3: Overall Coefficient

Assume U = 1,000 W/m^2/^{O}C

Step 4: Exchange Type and Dimensions

Using a horizontal exchanger, condense in the shell (1 Shell, 2 tube passes)

$$\Delta T_{lm} = \frac{\Delta T_1 - \Delta T_2}{\ln(\Delta T_1/\Delta T_2)}$$

$$\Delta T_{lm} = \frac{(250-80)-(54-32)}{\ln((250-80)/54-32)} = 72.38\ ^{O}C$$

Use 1 Shell pass and 2 tube passes, finding the temperature correction factor

$$R = \frac{250-54}{80-32} = 4.083$$

$$S = \frac{80-32}{250-32} = 0.22$$

From Figure 27, $F_t = 0.85$

So $\Delta T_{lm} = 0.85 \times 72.38 = 61.52\ ^{O}C$

Step 5: Heat Transfer Area

$$Q = UA\Delta T_m$$

$$A_o = \frac{Q}{U_{o,ass} \times \Delta T_{lm}}$$

$$A_o = \frac{(1.336 \times 10^7/1000)}{1{,}000 \times 61.52} = 60.32\ m^2$$

Step 6: Layout and Tube Size

1. Using Split-ring floating head exchanger for efficiency and case of cleaning.
2. For high pressure, using stainless steel 304 for shell and tube.
3. Using 19.05 mm outside diameter, 14.83 mm inside diameter and 5 m long tube (a popular size)
4. Triangular 23.81 mm pitch (pitch/diameter = 1.25)

Step 7: Number of Tubes

Area of one tube (neglecting thickness of tube sheets)

$$A = \pi \times 19.05 \times 10^{-3} \times 5 = 0.3\ m^2$$

Number of tubes = $\frac{60.32}{0.2992} = 201.6$, say 204

So, for 2 tube passes, tubes per pass = 102

Check the tube-side velocity

Tube Cross-sectional area = $\frac{\pi}{4} \times (14.83 \times 10^{-3})^2 = 0.0001727\ m^2$

So, area per pass = 102 × 0.0001727 = 0.0176 m^2

Volumetric Flow rate = 1.875×10^{-2} m^3/s

Tube-side velocity, $u_t = 1.875\times10^{-2}/0.0176 = 1.053$ m/s

The velocity is satisfactory, between 1-2 m/s. So, it is satisfactory.

Step 8: Bundle and Shell Diameter

From Table 5, for 2 tube passes, K_1=0.249, n_1=2.207

So $$D_b = d_o(\frac{N_t}{K_1})^{\frac{1}{n}} = 19.05(\frac{204}{0.249})^{\frac{1}{2.207}} = 398.1\ mm$$

For a Split-ring floating head exchanger the typical shell clearance from Figure 26 is 53 mm.

So, the shell side diameter = 398.1 + 53 = 451.1 mm

Step 9: Tube-side Coefficient

$$h_i = \frac{4200(1.35 + 0.02t)u_t^{0.8}}{d_i^{0.2}}$$

$$h_i = \frac{4200(1.35 + 0.02(56))(1.064)^{0.8}}{(14.83\times10^{-3})^{0.2}} = 2.531\times10^4$$

Step 10: Shell-Side Coefficient

Estimate tube wall temperature, Tw; assume condensing coefficient of 1,500 $W/m^2/^oC$

Mean Temperature Shell side = (250+53)/2 = 152 ^oC

Tube side = (80+32)/2= 56 ^oC

From $h_i\times(t_w - t) = U_{o,ass}(T - t)$

$1500\times(t_w - 56) = 1000(152 - 56)$

$t_w = 120$

Physical Properties at 120 ^oC

$$\mu_L = 0.232\times10^{-3}\frac{kg}{m\times s}$$

$$\rho_L = 994.3\frac{kg}{m^3}$$

$$k_L = 0.683\frac{W}{m\times K}$$

$$\rho_v = 1.121\frac{kg}{m^3}$$

Number of tubes in the center row $N_r = D_b/P_T = 398.1/1.25/19.05 = 17$

But Nr can be taken as two-third of the number in the central tube row Nr=2/3×17 = 11.

$$\text{From } \Gamma_h = \frac{m}{L \times N_t} = \frac{5190}{5 \times 204 \times 3600} = 1.413 \times 10^{-3} \ \frac{kg}{s \times m}$$

Using Kern's method, the mean coefficient for a tube bundle is given by:

$$h_o = 0.95 \times k_L \times \left(\frac{\rho_L \times (\rho_L - \rho_v) \times g}{\mu_L \times \Gamma_h}\right)^{-1/3} \times N_r^{-1/6}$$

$$h_o = 0.95 \times 0.683 \times \left(\frac{943.4 \times (943.4 - 1.121) \times 9.81}{0.232 \times 10^{-3} \times 1.413}\right)^{-1/3} \times 11^{-1/6} = 12990$$

It is significant lower than the assumed value of 1,500 $W/m^2/^OC$.

So, repeat calculation using new trial value of 12,990 $W/m^2/^OC$.

$h_o = 12603$ $W/m^2/^OC$. Close enough to estimate.

Step 11: Overall Heat Transfer Coefficient

1. k_w for stainless steel 304 = 26 $W/m^2/K$
2. Fouling factor of steam = 0.0005 $W/m^2/K$
3. Fouling factor of CCW with inhibitor = 0.0009 $W/m^2/K$

From equation,

$$\frac{1}{U} = \frac{1}{h_o} + \frac{1}{f_o} + \frac{d_o \ln(\frac{d_o}{d_i})}{2k_w} + \frac{d_o}{d_i} \times \frac{1}{f_i} + \frac{d_o}{d_i} \times \frac{1}{h_i}$$

U = 549 $W/m^2/k$

Significant lower than the assumed value of 1000 $W/m^2/K$. So, repeat the calculation using new trial value of 549 $W/m^2/K$

U = 553 $W/m^2/K$

Step 12: Pressure Drop

Shell Side Pressure Drop

Use pull-through floating head, no need for close clearance.

Select baffle spacing = shell diameter, 45 percent cut.

Use **Kern's method** to make an approximate estimate.

Cross-flow area, $A_s = \frac{(p_t - d_o)}{p_t} D_s l_B$

$$= \frac{(0.0238 - 0.019)}{0.0238} \times 0.617 \times 0.617 = 0.0762 \ m^2$$

Mass flow rate, based on inlet conditions, $G_s = \frac{5190}{3600} \times \frac{1}{0.0762} = 18.9 \frac{kg}{s \times m^2}$

Equivalent diameter, $d_e = \frac{1.27}{d_o}(p_t^2 - 0.917 d_o^2)$

$$= \frac{1.27}{0.019}\left(0.0238^2 - 0.917(0.019^2)\right) = 0.0156\, m$$

Reynolds number, $Re = \frac{\rho d_e u_s}{\mu} = \frac{4.119 \times 0.0156 \times 4.59}{1.47 \times 10^{-5}} = 20100$

From Figure 31, $j_f = 2.95 \times 10^{-2}$

$$u_s = \frac{G_s}{\rho_v} = \frac{18.9}{4.119} = 4.59\, m/s$$

Take pressure drop as 50 percent (pressure loss only be significant with gases) of that calculated using the inlet flow; neglect viscosity correction.

$$\Delta P_s = \frac{1}{2}(8 \times j_f \times \frac{D_s}{d_e} \times \frac{L}{l_B} \times \frac{\rho u_s^2}{2})$$

$$\Delta P_s = \frac{1}{2}\left(8 \times 2.95 \times 10^{-2} \times \frac{0.617}{0.0156} \times \frac{5}{0.617} \times \frac{4.119 \times 4.59^2}{2}\right) = 3.28\, kPa$$

$$= 0.0328\, bar$$

Tube Side Pressure Drop

Reynolds number, $Re = \frac{\rho d_i u_t}{\mu} = \frac{971 \times 1.48 \times 10^{-2} \times 1.095}{5.04 \times 10^{-4}} = 31300$

From Figure 28, $j_f = 3.65 \times 10^{-3}$

Neglect viscosity correction.

$$\Delta P_s = N_p(8 \times j_f \times \frac{L}{l_B} + 2.5) \times \frac{\rho u_t^2}{2}$$

$$\Delta P_s = 4 \times (8 \times 3.65 \times 10^{-3} \times \frac{5}{0.617} + 2.5) \times \frac{971 \times 1.095^2}{2} = 28.79\, kPa = 0.2879\, bar$$

Appendix C

Scrubber Design Calculation

Appendix C shows the sample scrubber design calculation which is packed bed type.

Mass and Compositional Balances

The gas is flown in the bottom of the tower and the liquid is flown in the top of the tower.

Assume that benzoic acid is absorbed by 90 wt%.

The data was calculated by sodium benzoate solution instead benzoic acid.

The given data are $y_1 = 0.137, x_2 = 0,\ V_1 = 11.01\frac{kg}{h}, m = 0.638\ (Solubilibty\ of\ NaBA)$

Then $V' = V_1(1 - y_1) = 11.01(1 - 0.137) = 9.5\ kg/h$

Moles benzoic acid in V1 are 1.51 kg/h. It is design to absorb of 90% benzoic acid. So benzoic acid at outlet is 0.1(1.51) = 0.151 kg/h. $V_2 = V' + 0.151 = 9.5 + 0.151 = 9.651\frac{kg}{h}. y_2 = \frac{0.151}{9.651} = 0.0156.$

The operating line for minimum liquid flow L_{min} is calculated by $x_{1max} = y_1/m = 0.137/0.638 = 0.2149$.

Substituting into the operating-line equation and solving for L_{min},

$$L'\left(\frac{x_2}{1-x_2}\right) + V'\left(\frac{y_1}{1-y_1}\right) = L'\left(\frac{x_1}{1-x_1}\right) + V'\left(\frac{y_2}{1-y_2}\right)$$

$$L'_{min}\left(\frac{0}{1-0}\right) + 9.5\left(\frac{0.137}{1-0.137}\right) = L'_{min}\left(\frac{0.2149}{1-0.2149}\right) + 9.5\left(\frac{0.0156}{1-0.0156}\right)$$

Solve the equation; $L'_{min} = 4.96\ kg/h$. Using $1.5L'_{min}, L' = 7.44\ kg/h$. Using $L' = 7.44$ in equation above and solving for the outlet concentration, $x_1 = 0.154$

Pressure Drop and Tower Diameter

Molecular weight of benzoic acid = 122 g/mol

Molecular weight of hydrogen = 2 g/mol

The gas average mol wt is 122(0.137)+2(1-0.137) = 18.46 g/mol

Density of gas,ρ_G

From equation PV=nRT

$$\rho = \frac{m}{V} = \frac{P \times mW}{RT} = \frac{39.96 \times 18.46}{0.00008314 \times (273.15+54) * 1000} = 27.12 \frac{kg}{m3}$$

Water viscosity $\mu = 0.000314\ Pa \times s$

Water density $\rho = 985.2\ kg/m^3$

Water kinematic viscosity $v = \frac{\mu}{\rho} = 0.319\ centistokes$

From Table 6, for 0.50 in. Berl Saddles (Ceramic), F_P=240 ft^{-1}. At a packing factor of 60 or higher, the pressure drop at flooding can be taken as 2.00 inH_2O/ft.

Assume diameter of packed column is 0.42 m

So, $G_L = \frac{L_2}{A} = \frac{7.44}{\pi \times \frac{0.42^2}{4}} = 53.7$ and $G_G = \frac{V_1}{A} = \frac{11.01}{\pi \times \frac{0.42^2}{4}} = 79.47$

Then $\frac{G_L}{G_G} = 0.676$

The flow parameter for Figure 38 is

$$\left(\frac{G_L}{G_G}\right)\left(\frac{\rho_G}{\rho_L}\right)^{0.5} = 0.676 \times (27.12/985.2)^{0.5} = 0.112$$

Using Fig 10.6-5, for a flow parameter of 0.112 (abscissa) and a pressure drop of 2.0 in./ft at flooding, a capacity parameter (ordinate) of 1.54 is read off the plot. Then, substituting into the capacity parameter equation and solving for v_G,

$$1.54 = v_G \left(\frac{\rho_G}{\rho_L - \rho_G}\right)^{0.5} F_P^{0.5} v^{0.05}$$

$$1.54 = v_G \left(\frac{27.12}{985.2 - 27.12}\right)^{0.5} 240^{0.5} 0.319^{0.05}$$

$$v_G = 0.626\ ft^2/s$$

Then $G_G = v_G \rho_G = 1.06 \frac{lb}{s \times ft^2}$ at flooding. Using 50% of the flooding velocity for design, $G_G = 0.5(1.06) = 2.12 \frac{lb}{s \times ft^2}$ $(0.022 \frac{kg}{s \times m^2})$. Also, the liquid flow rate G_L=$0.676 G_G$=$1.433 \frac{lb}{s \times ft^2}$ and the new capacity parameter is 0.5(1.54) = 0.77. Using this value of 0.77 and the same flow parameter, 0.112, a value of 0.13 in.water/ft is obtained from Figure 38.

The tower cross-sectional area = $11.01 \frac{kg}{h} \times \frac{1h}{3600s} \times \frac{1}{0.022} \frac{s \times m^2}{kg} = 0.137\ m^2$

So, Diameter = 0.417 m. which round up to 0.42 and the new tower cross-sectional area is 0.14 m^2

Estimation of H_{OG} by using Cornell's method.

Cornell's Method

$$D_L = 3.89\times10^{-10}\ m^2/s$$

$$D_v = 4.17\times10^{-4}\ m^2/s$$

$$\mu_v = 0.00126\ Ns/m^2$$

$$Sc_v = \frac{\mu_v}{\rho_g \times D_v} = \frac{0.00126}{27.12\times4.17\times10^{-4}} = 0.11$$

$$Sc_L = \frac{\mu_L}{\rho_L \times D_L} = \frac{0.315}{985.2\times3.89\times10^{-10}} = 82.10$$

$$L_W^* = \frac{Liquid\ mass\ flow\ rate}{Area\ colun\ corss-sectional\ area} = \frac{7.44}{0.137} = 53.76\ kg/ms^2$$

From Figure 39, at 50% flooding, K_3= 0.95

From Figure 40, at 50% flooding, Ψ_h = 54

From Figure 41, at L_W^* = 53.76, ϕ_h = 0.05

H_{OG} can be expected to be around 0.5 m, so as a first estimate Z can be taken as 0.5 m.

$$H_L = 0.305\phi_h {Sc_L}^{0.5} K_3 (\frac{Z}{3.05})^{0.15} = 0.305\times0.05\times82.10^{0.5}\times0.95\times(\frac{0.5}{3.05})^{0.15}$$
$$= 0.1\ m$$

As the liquid temperature, has been taken as 50 ^{O}C, and the liquid is water.

$$f_1 = (\frac{\mu_L}{\mu_w})^{0.16} = (\frac{0.315}{1.002})^{0.16} = 0.83$$

$$f_2 = (\frac{\rho_w}{\rho_L})^{1.25} = (\frac{998.2}{988.1})^{1.25} = 1.01$$

$$f_3 = (\frac{\sigma_w}{\sigma_L})^{0.8} = (\frac{0.0728}{0.0608})^{0.16} = 1.15$$

$$H_G = 0.011\Psi_h {Sc_v}^{0.5} (\frac{D_c}{0.305})^{1.11} \left(\frac{Z}{3.05}\right)^{0.33} / (L_W^* f_1 f_2 f_3)^{0.5}$$

$$H_G = 0.011\times54\times{0.11}^{0.5}\times(\frac{0.42}{0.305})^{1.11}\times\left(\frac{0.5}{3.05}\right)^{0.33} / (53.76\times0.83\times1.01\times1.15)^{0.5}$$

$$H_G = 0.021$$

While $m\frac{G_m}{L_m} = 0.638\times\left(\frac{9.5}{7.44}\right) = 0.814$

So, $H_{OG} = H_G + m\frac{G_m}{L_m}H_L = 0.021 + (0.814\times0.1) = 0.103$

Then, the number of transfer units is given by

$$N_{OG} = \frac{1}{1 - m\frac{G_m}{L_m}} \ln\left[\left(1 - m\frac{G_m}{L_m}\right)\frac{y_1}{y_2} + m\frac{G_m}{L_m}\right]$$

$$N_{OG} = \frac{1}{1 - 0.814} \ln\left[(1 - 0.814)\frac{0.137}{0.0156} + (0.814)\right] = 4.8$$

Hence, the height of the packed column is 4.8×0.103 = 0.495 m (Round up to 0.5 m).

Heat Transfer between Liquid and Vapor

Gas mass flow rate = 11.01 kg/h

Heat capacity of hydrogen = 14.43 kJ/kg/K

Temperature inlet = 327.15 K

Liquid mass flow rate = 7.44 kg/h

Heat capacity of liquid = 4.187 kJ/kg/K

Temperature inlet = 305.15 K

Temperature mixing = x K

$$Q = mc_p\Delta T$$

$$Q_{Hot} = Q_{Cold}$$

$$11.1\times14.43\times(327.15 - x) = 7.44\times4.187\times(x - 305.15)$$

Solve equation, x = 50 ^{O}C

Appendix D

Pressure Swing Adsorption Design

Appendix D shows the sample pressure swing adsorption design calculation.

Assumption

1. The data was based on *Dong-Kyu Moon Applied Energy 183(2016), 760-774.*
2. No hydrogen was adsorbed during a PSA operation.

The characteristics of the adsorption bed, adsorbents and operating conditions are shown in the Table D.

Table D Characteristics of the adsorption bed, adsorbents and operating conditions.

Adsorption bed		
Length, L (m)	1	
Adsorbent	**Zeolite LiX**	**Activated Carbon**
Type	Pellet	Cylindrical
Particle size, d_p (mm)	1.5-1.7	1.7-2.4
Particle density, ρ_p (g/cm^3)	1.050	0.750
Skeletal density, ρ_{sk} (g/cm^3)	2.000	1.850
Apparent density, ρ_b (g/cm^3)	0.7222	0.538
Bed porosity, $\varepsilon_b = (1 - \rho_b/\rho_p)$	0.312	0.283
Total porosity, $\varepsilon_t = (1 - \rho_b/\rho_{sk})$	0.639	0.709
Heat capacity, C_{ps} (J/kg K)	1070	1570
Pore volume (cm^3/g)	0.39	0.46
Total surface area (m^2/g)	664.7	1306.4
Operating Condition		
Flow rate, Q_{Feed} (SLPM)*	5	
Temperature, T_{Feed} (^{O}C)	35	
Adsorption Pressure, P_{AD} (bar)	35	
Desorption Pressure, P_{PG} (bar)	1.1	

Note: *A five-component hydrogen mixture gas (H_2: CO: N_2: CO_2 = 89:3:6:2 mol%)

The adsorbent bed packed with zeolite LiX flowed by activated carbon in the layered bed is used to separate between hydrogen and impurities which shown the breakthrough curves in Figure D.

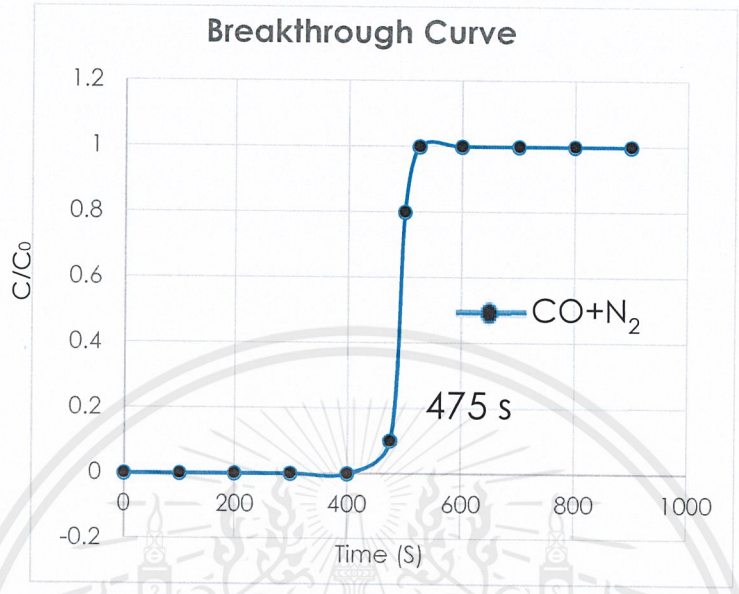

Figure D Breakthrough curve of activated carbon and zeolite LiX.

From Figure D the breakthrough point for removing carbon dioxide and nitrogen is 475 second.

In the scale-up, not only may it be necessary to change the column height, but also the actual throughput of fluid might be different from that used in the experimental laboratory unit. Since the mass velocity in the bed must remain constant for scale-up, the diameter of the bed should be adjusted to keep it constant. So, in this scale-up the feed compositions is assumed to be the same of feed composition in experiment. Then, adjust the diameter.

$$\frac{V_1}{\pi(D_1/2)^2} = \frac{V_2}{\pi(D_2/2)^2}$$

$$\frac{5}{\pi(0.021/2)^2} = \frac{705.18}{\pi(D_2/2)^2}$$

$$D_2 = 0.249\ m, say\ 0.25\ m$$

BIBLIOGRAHPY

Name: Mr. Siwat Valeekiatkul

Date of Birth: 27/10/1994

Address: 346, Sukhumvit Rd., Soi 10 (Onnut), Suangluang Bangkok 10250

E-mail: s.valeekiatkul@gmail.com

Academic Background:

1. 2010-2012 High school at Triam Udom Suksa Pattanakarn School
2. 2013-Present Taking up Bachelor of Petrochemical Engineering at King Mongkut's Institute of Technology Ladkrabang

Working Experience:

1. Project based industrial internship program at technologist section, Thai Oil Co., Ltd.
2. Co-operative education internship program at engineering section, Siam Mitsui PTA Co., Ltd.